Journal of Hazardous Materials 496 (2025) 139402

Contents lists available at ScienceDirect

Journal of Hazardous Materials

journal homepage: www.elsevier.com/locate/jhazmat

Advancing probabilistic risk assessment of perfluorooctanoic acid through integration of *in vitro* data and physiologically based toxicokinetic modeling coupled with population-specific analysis

Marija Opacic [a], Nemanja Todorovic [b], Mladena Lalic-Popovic [b], Bojana Stanic [a,*,1], Nebojsa Andric [a,*,2]

[a] University of Novi Sad, Faculty of Sciences, Department of Biology and Ecology, Serbia
[b] University of Novi Sad, Faculty of Medicine, Department of Pharmacy, Serbia

HIGHLIGHTS

- Benchmark concentrations (BMC) were calculated for PFOA-exposed human endothelial cells.
- BMC was transformed to apical and transcriptomic human equivalent doses (HED) using PBTK model.
- The lowest 10th percentile HED was below exposure level of the U.S. general population.
- Certain sensitive human populations could be at higher risk of PFOA exposure.
- Long-term low-level *in vitro* exposure coupled with PBTK modeling can be used for human risk assessment.

GRAPHICAL ABSTRACT

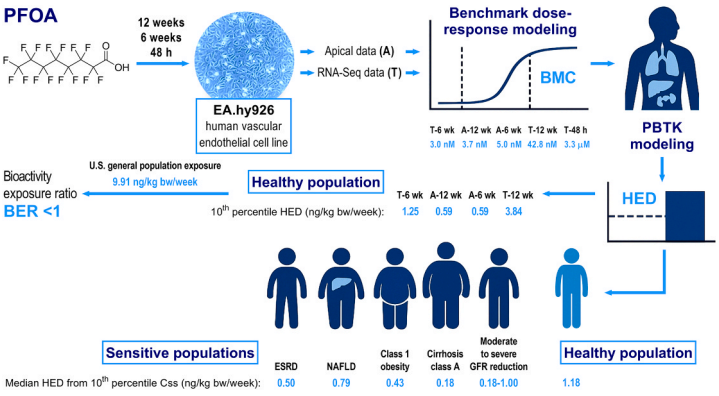

ARTICLE INFO

Keywords:
Perfluorooctanoic acid
Human endothelial cells
Human equivalent dose
Human physiologically based toxicokinetic model
Risk assessment

ABSTRACT

Current human health risk assessment for perfluorooctanoic acid (PFOA) has proven inadequate due to a lack of innovative approaches. Here, we applied benchmark dose-response modeling to derive benchmark concentrations (BMCs) for apical and transcriptomic changes in human endothelial cells EA.hy926 following both high-concentration short-term (48 h) and human-relevant long-term (6 and 12 weeks) PFOA exposures. BMCs were translated into human equivalent doses (HEDs) using a physiologically based toxicokinetic model. Long-term exposure produced sensitive biological responses: 10th percentile HEDs for apical and transcriptomic data were 0.59 and 3.84 ng/kg bw/week, respectively, both below the estimated U.S. general population exposure level (9.91 ng/kg bw/week). Predicted 10th percentile HED thresholds in individuals with certain conditions were: end-stage renal disease 0.50 ng/kg bw/week, moderate to severe reductions in glomerular filtration rate 0.18–1.00 ng/kg bw/week, cirrhosis class A 0.18 ng/kg bw/week, NAFLD 0.79 ng/kg bw/week, and class 1

* Correspondence to: University of Novi Sad, Faculty of Sciences, Department of Biology and Ecology, Trg Dositeja Obradovica 2, Novi Sad 21000, Serbia.
E-mail addresses: bojana.stanic@dbe.uns.ac.rs (B. Stanic), nebojsa.andric@dbe.uns.ac.rs (N. Andric).
[1] ORCID: 0000–0002-3049–4190
[2] ORCID: 0000–0003-1025–8358

https://doi.org/10.1016/j.jhazmat.2025.139402
Received 25 April 2025; Received in revised form 3 July 2025; Accepted 29 July 2025
Available online 30 July 2025

obesity 0.43 ng/kg bw/week, compared to healthy individuals (1.18 ng/kg bw/week), suggesting that PFOA can elicit adverse effects in endothelial cells at exposure levels below those currently experienced by the general population. Given the global prevalence of health conditions investigated in this study, a substantial portion of the population may face increased vulnerability to PFOA-induced health effects.

1. Introduction

Perfluorooctanoic acid (PFOA; IUPAC name: 2,2,3,3,4,4,5,5,6,6,7,7,8,8,8-pentadecafluorooctanoic acid, CAS# 335–67–1) is a synthetic chemical belonging to the class of per- and polyfluoroalkyl substances (PFAS). PFAS, including PFOA, have been widely synthesized and used in various industries and consumer products since the 1940s, but have recently gained attention as significant environmental contaminants [1]. In recent years, PFOA and other notable PFAS, such as perfluorooctanesulfonic acid (PFOS), have been phased out and replaced with alternative chemicals by major manufacturing companies [2]. Despite these efforts and because of their extreme persistence (often referred to as "forever chemicals"), PFAS continue to be found in both the environment and the human body, posing substantial risks to human and environmental health. Exposure to PFOA occurs through contaminated water, soil, air, and food, affecting humans, livestock, and wildlife alike. The mean serum concentration of PFOA in the United States (U.S.) general population is estimated at 1.38 ng/mL [3]. In a population exposed to PFAS-contaminated groundwater, the median serum concentration of PFOA was found to be 49 ng/mL, with an estimated half-life of approximately 2.36 years, shorter in women than in men [4]. Among adolescents and young adults exposed to high levels of PFAS through drinking water, PFOA exhibited the highest serum concentration, with a median value of 44.4 ng/mL [5]. A study of over 46,000 community residents aged 18 and older from the Mid-Ohio Valley, who had been exposed to various levels of PFOA through contaminated drinking water and food for decades, revealed a median blood PFOA level of 27 ng/mL, with concentrations ranging from as low as 0.25 ng/mL to nearly 18,000 ng/mL [6].

PFOA exposure is associated with a wide array of adverse health effects, including reproductive and developmental toxicity, hepatotoxicity, renal toxicity, immunotoxicity, neurotoxicity, genotoxicity, and carcinogenicity [7]. PFOA has also been shown to disrupt steroid hormone production and ovarian function, classifying it as a potential endocrine disruptor [8]. However, little is known about the effects of PFOA on human vascular endothelial cells and the vascular system in general. The inner lining of arteries, veins, and capillaries is made up of over one trillion endothelial cells that are continuously exposed to various stimuli, including environmental chemicals [9]. Increasing evidence suggests that exposure to harmful substances in the blood can lead to endothelial cell damage and, consequently, endothelial dysfunction. While studies have shown that other environmental chemicals, such as bisphenol A and phthalates, can adversely affect endothelial cells [10–16], research specifically focusing on the effects of PFOA on endothelial cells is limited. For instance, one study explored whether exposure to PFOA could induce morphological changes in the vascular 3D network structure [17], while other studies have examined the effects of PFOA on the plasma kallikrein-kinin system, which regulates vascular permeability [18], and whether gestational exposure to PFOA could inhibit early placenta development through the shrinkage of labyrinth vessels [19].

In recent years, new approach methodologies have been developed to accelerate chemical risk assessment. These methodologies include the use of sensitive and precise high-throughput analyses, *in silico* screening, novel *in vitro* models, long-term exposure studies, *in vitro*-to-*in vivo* extrapolation, and read across approach. Moreover, traditional methods such as the no-observed-adverse-effect level and lowest-observed-adverse-effect level have been largely replaced by benchmark dose (BMD) analysis, which provides a more precise estimate of chemical exposure that may lead to adverse effects. The BMD or its lower confidence limit (BMDL) obtained from the BMD analysis can be further used to calculate the human equivalent dose (HED). HED is then compared to the population exposure level to obtain the bioactive exposure ratio (BER). BER is a measure between exposure to a chemical and the estimate of biological activity for potential harm [20]. There are a number of *in vitro* studies aimed at obtaining benchmark concentrations (BMC) for different PFAS, including PFOA [21,22], which are then converted to human administered equivalent dose [23] or HED [24]. However, all these studies have used micromolar concentrations of PFOA for a relatively short exposure period (up to 14 days), which may limit the sensitivity of cellular responses and impact HED calculations. As a result, there is a need to explore the effects of long-term low-level exposures, more representative of real-life conditions, to improve the sensitivity and accuracy of risk assessments.

The permissible exposure limits and the tolerable daily and weekly intake (TWI) for PFOA have been established based on the data derived from animal and human studies. The European Food Safety Authority (EFSA) initially set a TWI of 6 ng/kg body weight (bw)/week in 2018 based on the data from human epidemiological studies regarding serum cholesterol levels [25], later revising it to 4.4 ng/kg bw/week in 2020, considering combined exposures to PFOA, perfluorononanoic acid, perfluorohexanesulfonic acid, and PFOS in adolescents, adults, elderly, and very elderly [26]. However, these values rely on broad population averages and do not adequately account for specific risk factors, such as body mass index and pre-existing health conditions, which may influence the kinetics of PFOA. Furthermore, these estimates do not fully address population-specific variations in chemical sensitivity, particularly among sensitive groups such as those with impaired kidney or liver function, obese, and others.

To address existing knowledge gaps and enhance risk assessment methodologies, this study integrates *in vitro* exposure data from the human macrovascular endothelial cell line EA.hy926 with physiologically based toxicokinetic (PBTK) modeling and population-specific analyses. The use of EA.hy926 cells as a model of the human endothelium, which is a critical yet understudied target tissue in PFAS toxicology, allowed us to explore potential vascular effects of PFOA. Given the endothelium's central role in cardiovascular health, our findings offer novel insights into PFOA-induced vascular toxicity and its long-term health implications. We implemented two exposure scenarios: short-term (acute) exposure with micromolar concentrations of PFOA and long-term (chronic) exposure with nanomolar concentrations, reflecting levels typically found in human plasma. The chronic, nanomolar exposure scenario offers a more realistic approximation of environmental exposure and is particularly relevant for detecting subtle cellular responses essential for deriving sensitive BMCs and corresponding HEDs. By analyzing traditional toxicological endpoints and toxicogenomic data, we calculated BMCs and derived HEDs using a PBTK model we developed for PFOA. This integrative approach enabled a comprehensive risk analysis across different population subgroups, including individuals with varying degrees of renal or hepatic impairment and those with obesity. Our findings suggest that these sensitive populations may be at increased risk of PFOA-induced endothelial dysfunction.

2. Material and methods

2.1. Chemicals

A full list of chemicals is provided in the Supplementary Material.

2.2. Cell culture

The human macrovascular endothelial cell line EA.hy926 was maintained as a monolayer culture at 37 °C in a humidified atmosphere containing 5 % CO_2, as previously described [11]. The complete culture medium consisted of Dulbecco's Modified Eagle's Medium supplemented with 10 % fetal bovine serum, 1 % penicillin-streptomycin solution, 1.5 g/L $NaHCO_3$, 0.11 g/L sodium pyruvate, 10 mM HEPES buffer, and 4 % HAT supplement (5 mM sodium hypoxanthine, 20 μM aminopterin, 0.8 mM thymidine). The medium was refreshed every three to four days, with subculturing performed when the cells reached ~90 % confluency. Cells were washed twice with phosphate-buffered saline (PBS) and then trypsinized using 0.25 % trypsin-ethylenediaminetetraacetic acid solution for 4 min. Following this, complete culture medium was added, and the cells were centrifuged at 400 × g for 5 min. The resulting suspension was mixed with Trypan blue solution and counted using an automated cell counter.

The human pro-monocytic cell line U937 was grown as a suspension culture at 37 °C in a humidified atmosphere with 5 % CO_2, as detailed in the Supplementary Material of our previous publication [15]. Cell suspensions at appropriate densities were utilized for both cell line propagation (up to 0.3×10^6 cells per mL) and for conducting the monocyte-endothelial adhesion assay following short-term (acute) and long-term (chronic) exposure of EA.hy926 cells to PFOA.

2.3. Short-term exposure of EA.hy926 cells to PFOA

EA.hy926 cells were cultured in 75 cm^2 flasks (BioLite™, Thermo Scientific) in complete culture medium under standard conditions. Cells were subcultured twice weekly – 1.8×10^6 cells were returned to the flasks on Mondays, and 2.8×10^6 cells on Fridays. For short-term exposure, EA.hy926 cells were plated in appropriate culture plates or dishes (BioLite™, Thermo Scientific), and 24 h after seeding exposed to either vehicle (0.05 % dimethyl sulfoxide, DMSO; 0 μM PFOA – control group) or three micromolar concentrations of PFOA (1 μM, 10 μM, and 100 μM – treatment groups) in complete culture medium for 48 h.

2.4. Long-term exposure of EA.hy926 cells to PFOA

Three different stock vials of EA.hy926 cells cryopreserved on different dates (biological replicates) were thawed and cultured in separate 25 cm^2 flasks (BioLite™, Thermo Scientific) under standard conditions for two weeks. The cells from each flask were then divided into four flasks, resulting in a total of 12 flasks. Over the subsequent 12 weeks, EA.hy926 cells were subcultured twice a week – 0.75×10^6 cells per flask were replated on Fridays, and 0.95×10^6 cells on Tuesdays. Three h after seeding, cells were exposed to either vehicle (0.05 % DMSO; 0 nM PFOA – control group) or three nanomolar concentrations of PFOA (1 nM, 10 nM, and 100 nM PFOA – treatment groups) (Supplementary Figure 1). As specified in certain experiments, treatments were also continued in cell culture plates and dishes.

2.5. Apical endpoints

The following apical endpoints were analyzed after short-term and long-term exposure of EA.hy926 cells to PFOA: cell viability, apoptosis and necrosis, cell cycle progression, endothelial permeability, monocyte adhesion to the endothelial cell monolayer, cell adhesion to the extracellular matrix, cell migration, endothelial tube formation, and the production of reactive oxygen species (ROS). Detailed protocols for these assays are provided in the Supplementary Material.

2.6. Transcriptomics

For short-term exposure, EA.hy926 cells were plated in 35-mm dishes (0.6×10^6 cells per dish; Nunc™, Thermo Scientific) and exposed to either vehicle (0.05 % DMSO; 0 μM PFOA – control group) or three micromolar concentrations of PFOA (1 μM, 10 μM, and 100 μM PFOA – treatment groups) the following day. After 48 h of exposure, the cells were rinsed with PBS, collected in 0.5 mL of TRIzol, and the RNA was extracted afterward. In long-term exposure experiments, EA.hy926 cells originating from each flask after 6 and 12 weeks of continuous exposure to either vehicle (0.05 % DMSO; 0 nM PFOA – control group) or three nanomolar concentrations of PFOA (1 nM, 10 nM, and 100 nM PFOA – treatment groups) were collected directly during subculturing on Fridays into clean RNase-, DNase-, and pyrogen-free 1.5 mL microcentrifuge tubes (~1×10^6 cells per tube). Cells were centrifuged at 400 × g for 5 min, rinsed with PBS, centrifuged again, and stored in 0.5 mL of TRIzol at –80 °C for subsequent RNA isolation. Three replicates of control and each treatment group per experiment were submitted to BGI Europe (Warsaw, Poland) for mRNA sequencing (RNA-Seq) and further analysis. RNA quantity and integrity were assessed using an Aglient 4150 Bioanalyzer (Agilent Technologies, Santa Clara, CA, USA). All samples had an RNA integrity number greater than 9.5, indicating very high quality. RNA-Seq was conducted on the DNBSEQ platform, with sequencing length PE150 and an average yield of 6.65 G data per sample. Sample reads were trimmed to remove any reads with more than 5 % unknown base content, along with adapters and low-quality bases. HISAT was used to align the clean reads to the reference genome (species: *Homo sapiens*; source: NCBI; reference genome version: GRCh38.p14, https://www.ncbi.nlm.nih.gov/datasets/genome/GCF_000001405.40/, accessed 18 October 2024), while Bowtie2 was used to align the clean reads to reference genes. The average alignment ratio of the sample comparison genome was 98.74 %, whereas the average alignment of the gene set was 85.92 %; a total of 18048 genes were detected. The analysis of differentially expressed genes (DEGs) was performed by BGI using the DESeq2 method [27].

2.7. BMC modeling

BMC modeling was conducted on two sets of data: apical endpoints and log2-transformed DESeq2 normalized gene counts using the BMDExpress3 [28] available at https://github.com/auerbachs/BMDExpress-3. The data were pre-filtered using the Williams Trend Test with 500 permutations, a linear 1.5-fold change, and a significance threshold of $p < 0.05$ to select the probes with monotonic dose responses. Probes passing the Williams Trend Test were further modeled using the U.S. Environmental Protection Agency's (EPA) BMDS online tool (https://bmdsonline.epa.gov/) with the following parameters: benchmark response (BMR) type as standard deviation (SD) with a BMR factor of 1 SD, model selection for BMC, BMCL, and upper confidence limit of the BMC (BMCU) in the best model (Linear, Exp3, Exp5, Poly2, Hill), and best polynomial model test using Nested Chi-Square, with a *p*-value cut-off of 0.05. The BMC data were further filtered based on the following criteria: BMC greater than the concentrations used in the analysis and the BMCU to BMCL ratio greater than 40. Gene accumulation plot was created in BMDExpress3, while density plots were created using the R program.

2.8. PBTK modeling

A PBTK model for PFOA was developed utilizing previously published models [29–31]. Toxicokinetic modeling of PFOA is inherently complex due to the limited or incomplete *in vivo* data necessary for model validation. However, human pharmacokinetic data for PFOA are available from the open-label clinical study conducted by Elcombe et al.,

which investigated the anticancer effects of PFOA [32]. The study results, including plasma PFOA concentrations, are detailed in the associated patent publication. These data have not been previously used for the validation of a PFOA-specific PBTK model. GastroPlus™ software (version 9.9, SimulationPlus Inc., USA) was used for PFOA PBTK modeling. PFOA-specific input parameters are summarized in Table 1. The molecular structure of PFOA was generated using ChemDraw software (version 20.0, PerkinElmer Informatics). The toxicokinetics of PFOA has not been thoroughly investigated and the existing literature reveals inconsistencies in the reported findings. Notably, previous studies suggest a prolonged elimination half-life ranging between 0.5 and 1.5 years [33]. The extended elimination half-life complicates the modeling process and the determination of steady-state concentrations (Css) during repeated dosing, due to software limitations that restrict population kinetics monitoring for PFOA to a maximum of 16,000 h. To address this limitation, we adjusted the clearance rate in our model to minimize the elimination half-life, ensuring that it remained within the previously reported, realistic ranges.

The model validation was carried out using three different doses of PFOA (100 mg, 300 mg, and 750 mg), as shown in Table 2. The model exploration included conducting a Parameter Sensitivity Analysis (PSA) and evaluating pharmacokinetic profiles based on different dosage forms and the persistence of food in the gastrointestinal tract. A comparative analysis was conducted between immediate-release (IR) capsules, as used in the clinical study, and an IR solution, which may represent a potential environmental source of PFOA. PSA was performed to identify key parameters with the greatest impact on model outcomes. The validated model was utilized to predict the HED. The BMC was used as aimed PFOA plasma concentration, without the need for additional calculations, as these values were derived from an endothelial cell line. In other words, the plasma concentration of PFOA corresponds directly to its concentration in the cell culture medium. The input dose was adjusted until the $c_{16,000}$ value reached or exceeded the BMC.

2.9. Gene enrichment analysis

Pathway analysis of genes with calculated BMCs was performed using the Reactome pathway database tool (https://reactome.org). The pathways were sorted from the lowest to the highest false discovery rate (FDR) value. Five pathways with the lowest FDR value for each concentration of PFOA were presented using the ggplot2 package in R.

Table 1
Input parameters in human PBTK model for PFOA.

Parameter	Value	Source
Molecular weight (g/mol)	414.07	ADMET predictor
log D (pH 7.4)	1.158	ADMET predictor
pKa	1.3 (acid)	ADMET predictor
Human jejunal permeability ($\times 10^{-4}$ cm/s)	4.16	ADMET predictor
Dose (mg)	100, 300, 750 (p.o. capsule)	(Elcombe et al., 2011)
Water solubility at 37 ℃ (mg/mL)	9.03	Experimentally determined
Mean precipitation time (s)	900	GastroPlus™ default value
Diffusion coefficient ($\times 10^{-5}$ cm^2/s)	0.88	GastroPlus™ calculated value
Drug particle density (g/mL)	1.2	GastroPlus™ default value
Effective particle radius (μm)	25	GastroPlus™ default value
Shape factor	4.00	GastroPlus™ default value
Blood/plasma conc. ratio	0.88	ADMET predictor
Unbound percent in plasma (%)	0.02	ADMET predictor
Clearance, CL (mL/min/kg)	0.0002	(Dourson and Gadagbui, 2021)
Volume of distribution, V_c (L)	12.994	GastroPlus™ calculated value
Elimination half-life (h)	9004.973	GastroPlus™ calculated value
Simulation time (h)	16,000	GastroPlus™ calculated value

Table 2
In vivo data from the study by Elcombe et al. (2011).

Dosage form	Dose	Additional data
p.o. capsule	100 mg	Fasted state, two male and one female patients, average age 62 (min 48, max 70)
p.o. capsule	300 mg	Fasted state, three male and one female patients, average age 61 (min 50, max 74)
p.o. capsule	750 mg	Fasted state, two male and one female patients, average age 65 (min 60, max 68)

2.10. BER calculation

The U.S. population's 95th percentile serum PFOA concentration (3.57 ng/mL), obtained from the National Health and Nutrition Examination Survey (NHANES; 2017–March 2020) and reported by Botelho et al. [3], was used as the target plasma concentration in our PBTK model. To determine the corresponding external dose, we iteratively adjusted the administered weekly dose of PFOA in the model until the predicted venous plasma Css matched the target value of 3.57 ng/mL. This approach yielded a modeled HED of 9.91 ng/kg bw/week, which we used as the reference exposure value for subsequent bioactivity BER calculations according to the approaches described by Rowan-Carroll et al., with minor modifications [23]. In Approach 1, the lower bound 10th percentile HED was rounded to the nearest integer and compared to the estimated exposure level of the U.S. general population. In Approach 2, the median HED of genes associated with pathways was calculated and the HED of the most sensitive pathway was similarly compared to the estimated weekly exposure level of the U.S. general population.

2.11. Statistical analysis

Statistical analysis of apical data was conducted using the Prism 8 software package (GraphPad Software, Inc., La Jolla, CA, USA) by one-way analysis of variance (ANOVA) with Dunnett's multiple comparisons post-hoc test, while *t*-test with one-tailed distribution and two-sample equal variance was used for the data presented in Table 5. A *p*-value of < 0.05 was considered significant.

3. Results

3.1. Apical endpoints

3.1.1. Apoptosis and necrosis

Both short-term and long-term exposure of EA.hy926 cells to PFOA did not affect cell viability across any of the tested concentrations (Supplementary Figure 2). However, the 12-week exposure to 100 nM PFOA resulted in approximately a 17 % reduction in cell proliferation (data not shown). To further investigate the effects of PFOA, we examined whether short-term and long-term exposures induced apoptosis or necrosis in EA.hy926 cells. As illustrated in Fig. 1, short-term exposure to 1 μM, 10 μM, and 100 μM PFOA did not trigger either apoptosis or necrosis. On the other hand, we noted a decline in live cell counts after 6 weeks of exposure to 1 nM PFOA and after 12 weeks of exposure to 1 nM, 10 nM, and 100 nM PFOA. The number of apoptotic cells increased only after 12 weeks of exposure to 1 nM and 100 nM PFOA. Additionally, necrotic cell counts rose after 6 weeks of exposure to 1 nM PFOA and after 12 weeks at all three concentrations of PFOA (Fig. 1A and B).

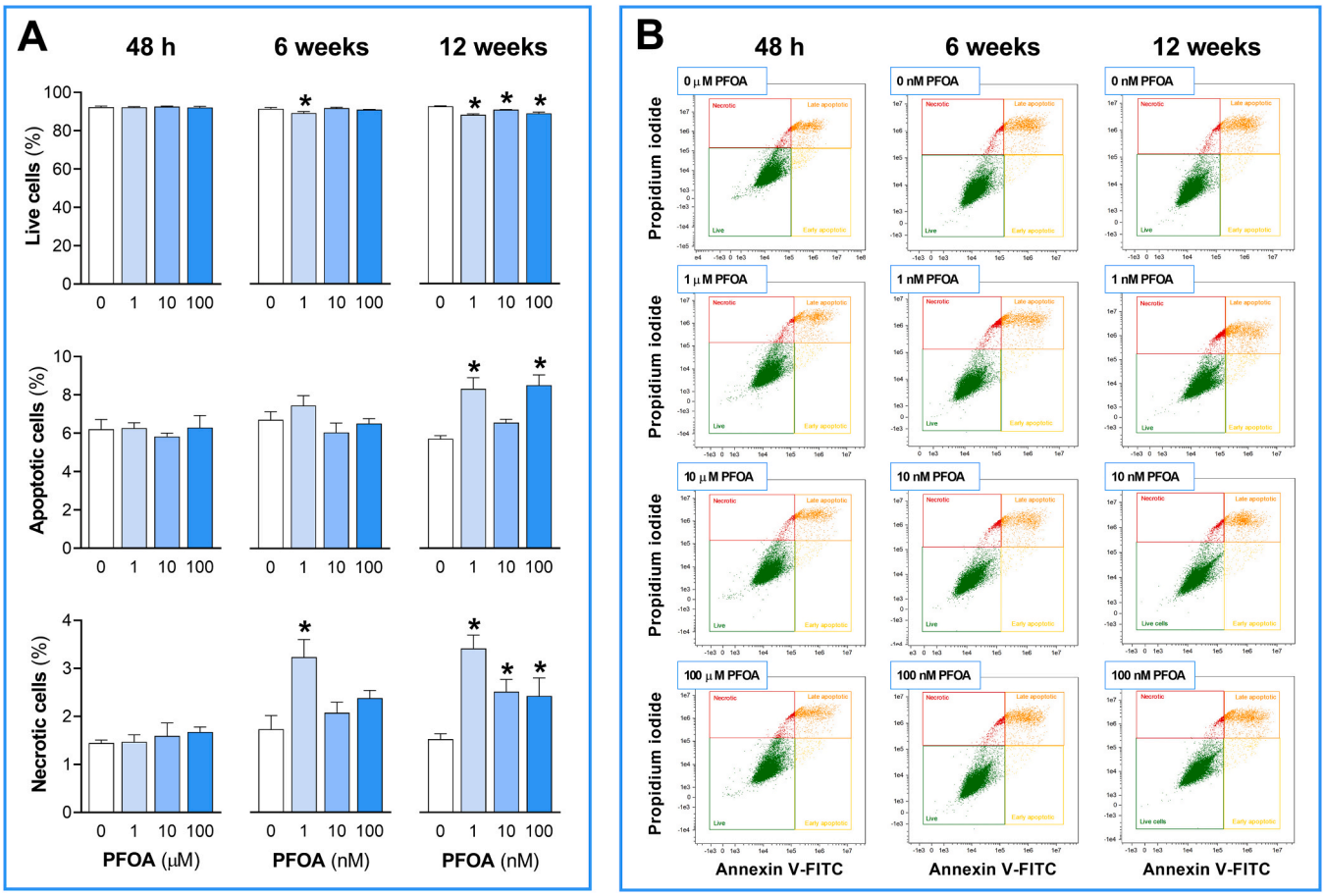

Fig. 1. The effect of short-term and long-term exposure of EA.hy926 cells to PFOA on apoptosis and necrosis. EA.hy926 cells were exposed to 1 μM, 10 μM, and 100 μM PFOA or vehicle (0.05 % DMSO; 0 μM PFOA) for 48 h (short-term exposure) and 1 nM, 10 nM, and 100 nM PFOA or vehicle (0.05 % DMSO; 0 nM PFOA) for 6 and 12 weeks (long-term exposure), followed by the assessment of apoptosis and necrosis using annexin V–fluorescein isothiocyanate (FITC) and propidium iodide (PI) on a flow cytometer. (A) The results were expressed as the percentage of live, apoptotic, and necrotic cells. Each data bar represents the mean ± SEM of 4 independent experiments (short-term exposure) or 3 cell culture flasks (long-term exposure). (B) Representative dot-plots from flow cytometry are shown. *$p < 0.05$ *vs.* control.

3.1.2. *Cell cycle*

Exposure of EA.hy926 cells to PFOA for 48 h and 6 weeks had no impact on cell cycle progression across any of the tested concentrations. However, after 12 weeks of exposure to 100 nM PFOA, we observed a decrease in the percentage of cells in the G_0/G_1 phase and a corresponding increase in the S phase, but the percentage of cells in the G_2/M phase remained comparable to the control group. Notably, the percentage of cells in the G_2/M phase was significantly elevated following 12 weeks of exposure to 10 nM PFOA (Fig. 2 and Supplementary Figure 3).

3.1.3. *Endothelial permeability and monocyte adhesion to endothelial cell monolayer*

A significant increase in endothelial permeability was noted only after 12 weeks of exposure of EA.hy926 cells to 1 nM, 10 nM, and 100 nM of PFOA (Fig. 3A), whereas monocyte adhesion to the endothelial cell monolayer significantly increased after 6 weeks of exposure to 10 nM PFOA and after 12 weeks of exposure to 100 nM PFOA (Fig. 3B and C).

3.1.4. *Cell migration and endothelial tube formation*

We next examined angiogenesis-related processes, including endothelial cell adhesion to the extracellular matrix (ECM), cell migration, and endothelial tube formation. Both short-term and long-term exposure of EA.hy926 cells to PFOA did not affect adhesion to fibronectin at any of the tested concentrations (Supplementary Figure 4). However, cell migration increased after 6 weeks of exposure to 10 nM and 100 nM PFOA but decreased after 12 weeks of exposure to 100 nM PFOA (Fig. 4A, Supplementary Figure 5 A). Endothelial tube formation was affected only after 12 weeks of exposure to 10 nM and 100 nM PFOA. We observed a significant increase in the total length of tubes, as well as a higher number of nodes and junctions, and greater total branching length, indicating enhanced endothelial tube formation (Fig. 4B, Supplementary Figure 5B). Additionally, we investigated ROS production following both short-term and long-term exposure to PFOA. The results showed significantly reduced ROS levels after 6 weeks of exposure to 10 nM and 100 nM PFOA (Supplementary Figure 6).

3.2. *Identification of DEGs*

Whole-genome transcriptome analysis identified DEGs in EA.hy926 cells, with at least a 2-fold change and a Q value of ≤ 0.05, following both short-term and long-term exposure to specified concentrations of PFOA (Fig. 5A). The number of DEGs varied depending on the duration of exposure and the concentration of PFOA. After 48 h, the highest number of DEGs was observed at the highest concentration of 100 μM PFOA, resulting in 359 DEGs (119 upregulated, 240 downregulated). In contrast, exposure to 10 μM PFOA and 1 μM PFOA resulted in 197 DEGs (88 upregulated, 109 downregulated) and 98 DEGs (61 upregulated, 37 downregulated), respectively. Interestingly, the greatest overall number

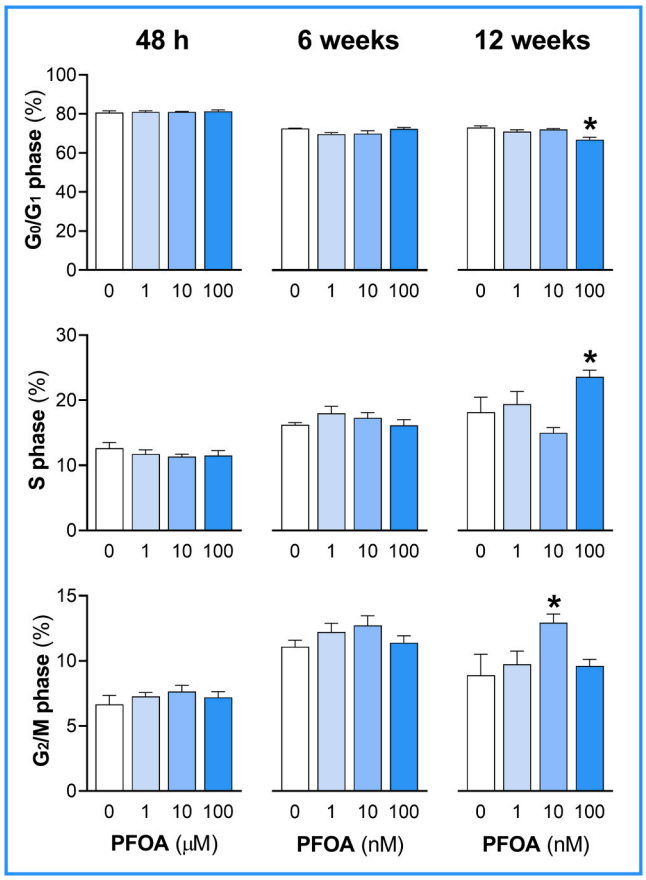

Fig. 2. The effect of short-term and long-term exposure of EA.hy926 cells to PFOA on cell cycle distribution. EA.hy926 cells were exposed to 1 μM, 10 μM, and 100 μM PFOA or vehicle (0.05 % DMSO; 0 μM PFOA) for 48 h (short-term exposure) and 1 nM, 10 nM, and 100 nM PFOA or vehicle (0.05 % DMSO; 0 nM PFOA) for 6 and 12 weeks (long-term exposure), followed by cell cycle analysis using PI on a flow cytometer. The results were expressed as the percentage of cells in G_0/G_1, S, and G_2/M phase. Each data bar represents the mean ± SEM of 4 independent experiments (short-term exposure) or 3 cell culture flasks (long-term exposure). *$p < 0.05$ *vs.* control.

of DEGs was detected after 6 weeks of exposure to 1, 10, and 100 nM PFOA, surpassing the counts from 48-h exposure to the higher micromolar concentrations and the 12-week exposure to the same nanomolar concentrations of PFOA. Notably, exposure to 10 nM PFOA for 6 weeks produced the highest total of 6018 DEGs, comprising 5038 upregulated and 980 downregulated genes. Conversely, exposure to 1 nM and 100 nM PFOA yielded 397 DEGs (311 upregulated, 86 downregulated) and 3811 DEGs (3504 upregulated, 307 downregulated), respectively. A similar trend was evident after 12 weeks of exposure to the three nanomolar concentrations of PFOA. Again, the highest number of DEGs was associated with 10 nM PFOA, with a total of 1725 DEGs (1627 upregulated, 98 downregulated). In comparison, exposure to 1 nM PFOA and 100 nM PFOA resulted in 205 DEGs (109 upregulated, 96 downregulated) and 904 DEGs (701 upregulated, 203 downregulated), respectively (Fig. 5B). The hierarchical clustering of DEGs is presented in Supplementary Figure 7.

3.3. Determination of BMC

To visualize changes in response to increasing concentrations of PFOA over different exposure durations (short-term – 48 h and long-term – 6 and 12 weeks) and levels of biological organization (apical – A and transcriptomics – T), we plotted accumulation curves for the BMC values (Fig. 6). The accumulation plots across three time points and two levels of biological organization displayed similar curve shapes, with the initial segments exhibiting shallow slopes across the BMCs, until reaching a dynamic response phase. Notably, after 48 h, changes in apical endpoints (A-48 h) did not show a concentration-dependent response to PFOA exposure.

The calculated median BMC values were as follows: 5 nM for A-6 weeks, 3.7 nM for A-12 weeks, 3.3 μM for T-48 h, 3.0 nM for T-6 weeks, and 42.8 nM for T-12 weeks. The median BMCL and BMCU values were determined as follows: for A-6 weeks, 3.7 nM and 12.1 nM; for A-12 weeks, 2.4 nM and 8.8 nM; for T-48 h, 2.1 μM and 7.6 μM; for T-6 weeks, 1.9 nM and 6.4 nM; and for T-12 weeks, 26.8 nM and 102.9 nM; respectively. Notably, the median BMC value for T-6 weeks was 14.3 times lower than that for T-12 weeks and ~1100 times lower than that for T-48 h. The median BMC values for A-6 weeks and A-12 weeks were comparable to that of T-6 weeks but were 8.5 times and 11.7 times lower than the median BMC value for T-12 weeks, respectively (Fig. 7).

The density plot curves of BMC indicate unimodal distributions for T-48 h and T-6 weeks, suggesting that the BMC values were positively skewed. In contrast, the T-12 weeks curve was bimodal, revealing two distinct subgroups of the BMC values (Supplementary Figure 8).

3.4. Pathway analysis

Next, we conducted pathway analysis using the genes with determined BMC values following short-term (48 h) and long-term (6 and 12 weeks) exposure of EA.hy926 cells to PFOA. Based on the FDR values, the top three pathways affected by short-term exposure to PFOA were "NGF-stimulated transcription", "Signaling by NTRKs", and "Nuclear events (kinase and transcription factor activation)". After 6 weeks of exposure, PFOA-affected genes were associated with the following top three pathways: "NGF-stimulated transcription", "Nuclear events", and "Interleukin-4 and Interleukin-13 signaling". After 12 weeks of exposure, "Interleukin-10 signaling" was the only affected pathway with high confidence (FDR = 0.053), whereas other pathways were with lower confidence (FDR = 0.34) (Fig. 8). We further determined whether the genes associated with pathways in each exposure scenario were upregulated or downregulated. After 48 h of exposure, all PFOA-affected genes were downregulated, whereas after 6 weeks of exposure, all affected genes, except one, were upregulated. On the other hand, the pathways affected by 12-week exposure to PFOA predominantly contain a mix of upregulated and downregulated genes.

3.5. PBTK model and determination of HED and BER

The developed PBTK model can be considered adequate, as it largely aligns with the clinical *in vivo* data (Supplementary Figure 9). The results of the PSA indicate that C_{max}, $AUC_{(0\text{-}t)}$, and Liver C_{max} are highly sensitive to variations in Cl: PFOA-kidney (L/h), the fraction of PFOA unbound in plasma, and to a lesser extent, Kp: PFOA-Adipose (Supplementary Figure 10). No significant differences were observed in the concentration-time profiles between the two forms, nor between the fasted and fed states (Supplementary Figure 11).

The PBTK model for PFOA and the BMC data from *in vitro* assays were used to determine the HED values. The variability in HEDs across different exposure scenarios was visualized using boxplots. As shown in Fig. 9, the A-HED from the 6-week exposure was derived only from one apical assay with the value at 0.59 ng/kg bw/week. The median A-HED from the 12-week exposure was determined to be 4.3 ng/kg bw/week, with the lower bound 10th percentile at 0.59 ng/kg bw/week. The lowest T-HED was obtained from the 6-week exposure, with the median value at 3.6 ng/kg bw/week and the lower bound 10th percentile at 1.25 ng/kg bw/week. The T-HEDs from the 12-week exposure were higher than those obtained after 6 weeks, with the median value at 48.5 ng/kg bw/week and the lower bound 10th percentile at 3.8 ng/kg bw/week. The highest T-HED value was obtained from the 48-h exposure, which accounts for a single exposure to PFOA, with the median

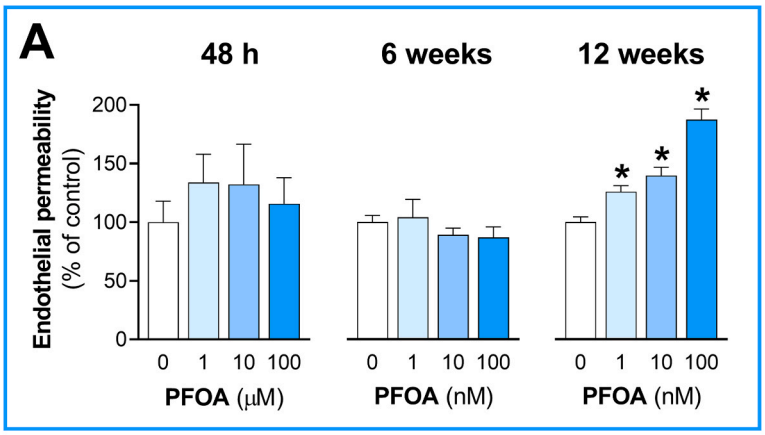

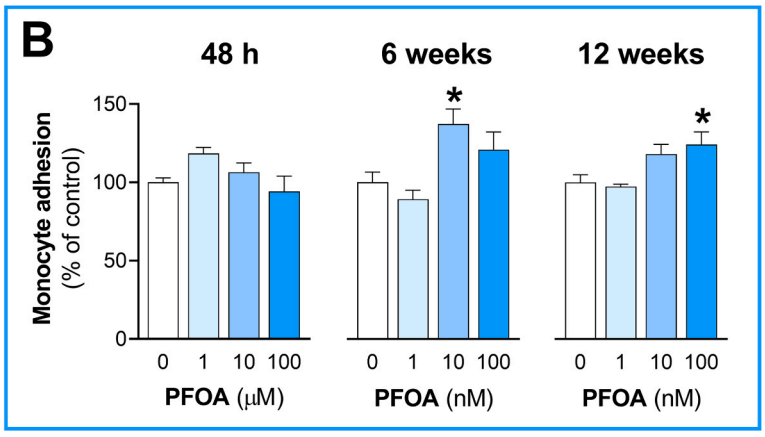

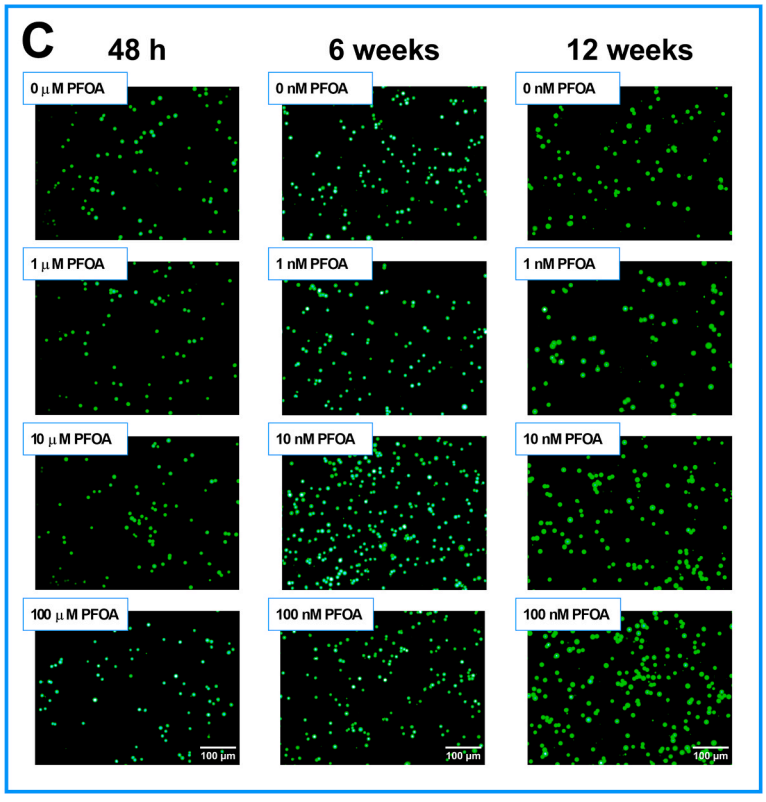

(caption on next page)

Fig. 3. The effect of short-term and long-term exposure of EA.hy926 cells to PFOA on endothelial permeability and monocyte adhesion to endothelial cell monolayer. EA.hy926 cells were exposed to 1 μM, 10 μM, and 100 μM PFOA or vehicle (0.05 % DMSO; 0 μM PFOA) for 48 h (short-term exposure) and 1 nM, 10 nM, and 100 nM PFOA or vehicle (0.05 % DMSO; 0 nM PFOA) for 6 and 12 weeks (long-term exposure), followed by the assessment of (A) endothelial permeability using the two-compartment permeability assay with FITC-labeled dextran and (B) the extent of monocyte adhesion to the EA.hy926 monolayer using calcein AM-labeled U937 cells. (A, B) The results were expressed relative to the vehicle-treated control (100 %). Each data bar represents the mean ± SEM of 4 independent experiments (short-term exposure) or 3 cell culture flasks (long-term exposure). (C) Representative fluorescent photomicrographs of calcein AM-labeled U937 cells adhered to the EA.hy926 cell monolayer are shown; scale bar 100 μm. *$p < 0.05$ *vs.* control.

value at 523 μg/kg bw/week and the lower bound 10th percentile at 144 μg/kg bw/week (data not shown).

The BER calculated from the apical data obtained after 6-week exposure of EA.hy926 cells to PFOA is 0.06. This value is below the calculated weekly exposure of the U.S. general population (9.91 ng PFOA/kg bw/week). The BER values calculated from the transcriptomic data using the lower bound 10th percentile of genes (Approach 1) were also below the calculated weekly exposure of the U.S. general population – 0.12 for the 6-week exposure and 0.39 for the 12-week exposure. The BER values calculated from the transcriptomic data using the median HED of the genes associated with the most sensitive pathway (Approach 2) were increased for both the 6-week exposure and the 12-week exposure and were 0.30 and 5.55, respectively, but were still below the calculated weekly exposure of the U.S. general population (Table 3).

We also calculated human HEDs and BERs for three genes – *IL1A*, *CXCL8*, and *KLF4* – which exhibited BMCs at both 6- and 12-week exposure time points (Table 4). These genes are well-established mediators of endothelial cell function, each associated with key Gene Ontology (GO) biological processes relevant to vascular biology, including angiogenesis, inflammatory signaling, and cellular responses to hemodynamic forces. In accordance with previously shown data, HED values for all three genes were lower after 6 weeks than after 12 weeks. For example, *IL1A* (encoding interleukin (IL)-1 alpha, a pro-inflammatory cytokine that also regulates vascular endothelial growth factor (VEGF) production) exhibited a HED of 3.13 ng/kg bw/week at 6 weeks (BER = 0.32) and 52.47 ng/kg bw/week at 12 weeks (BER = 5.29). Similarly, *CXCL8* (encoding IL-8, involved in endothelial chemotaxis and vascular remodeling) and *KLF4* (encoding Krüppel-like factor 4, a shear-responsive transcription factor with anti-inflammatory and angiostatic functions) showed significant transcriptional sensitivity and low BERs relative to the U.S. general population exposure (9.91 ng/kg bw/week).

In addition to these consistently responsive genes, we observed time point-specific changes in several other genes critical for endothelial cell function: *IL6* (encoding IL-6, a multifunctional cytokine involved in vascular inflammation that also regulates VEGF production), *IL1B* (encoding IL-1 beta, another key inflammatory mediator involved in positive regulation of tight junction disassembly, regulation of nitric oxide synthase activity, and numerous other processes in endothelial cells), and *VEGFA* (encoding VEGFA, a major regulator of angiogenesis and vascular permeability) at 6 weeks, and *RGCC* (encoding regulator of cell cycle RGCC, associated with negative regulation of angiogenesis, endothelial barrier integrity, and stress response) and *SELP* (encoding P-selectin, a cell adhesion molecule that mediates leukocyte-endothelial interactions) at 12 weeks of PFOA exposure (data not shown).

3.6. Determination of HED for different human populations

Next, we calculated median HEDs from different ranges of bioactive PFOA concentrations (taken as Css), obtained after 6-week exposure of EA.hy926 cells. This analysis was performed for the healthy population as well as for several sensitive populations, grouped into three categories: (i) population with renal impairment encompassing end-stage renal disease (ESRD) and severe, moderate, and mild decrease in glomerular filtration rate (GFR); (ii) population with hepatic impairment including three classes of cirrhosis according to the Child-Pugh (CP) classification (CP classes A, B, and C), simple steatosis, and non-alcoholic fatty liver disease (NAFLD); and (iii) population with class 1 obesity. Our analysis reveals that the 10th and 25th–75th percentile HED values for populations with ESRD, severe to moderate decreases in GFR, CP class A cirrhosis, NAFLD, and class 1 obesity were lower than those observed in the healthy adult population. Conversely, individuals with a mild decrease in GFR, CP class B and C cirrhosis, and simple steatosis exhibited higher 10th and 25th–75th percentile HED values. At the 90th percentile, no significant differences in HED values were observed between the sensitive and healthy populations, except for the CP class C cirrhosis subgroup (Fig. 10). Similar trends in HEDs were observed following 12-week exposure of EA.hy926 cells to PFOA (Supplementary Figure 12).

Table 5 summarizes the predicted HEDs after 6 weeks of PFOA exposure in populations with altered physiology, including individuals with varying degrees of renal or hepatic impairment and those with class 1 obesity, while Supplementary Table 1 provides the corresponding HEDs following a 12-week exposure. Collectively, the results indicate that sensitive populations may exhibit adverse effects at lower PFOA exposure levels than healthy individuals.

4. Discussion

Risk assessment of chemicals, including PFOA, presents several significant challenges. One of the primary issues, regardless of whether *in vitro* or *in vivo* approaches are used, is the sensitivity of biological responses to environmental chemical exposures. The BMC and the resulting HED, which guide safety evaluations for the general population, are highly influenced by the approach used to identify the most sensitive biological response. Additionally, a more comprehensive understanding of health risks in sensitive populations is essential to support more effective, evidence-based risk management decisions.

4.1. Sensitivity of cellular responses to PFOA between different exposure scenarios

Our study integrates BMC modeling with transcriptomic and apical endpoint data to evaluate the sensitivity of cellular responses to PFOA under different exposure scenarios (acute *vs.* chronic). A key finding is that chronic *in vitro* exposure to PFOA elicits a more sensitive response in human endothelial cells compared to acute exposure. Besides the fact that the BMC value for A-48h data could not be calculated, we also observed a significant shift in BMC values derived from the transcriptomics data following short- and long-term exposure of EA.hy926 cells to PFOA. Comparable shifts have been reported in human liver spheroid studies, where BMC values for PFOA decreased over time – from 21.9 μM at 24 h to 16.9 μM after 10 days of exposure [21], and from 40 μM at 24 h to approximately 7 μM after 14 days of exposure [23]. It should be noted that the shift in the BMC values calculated from the transcriptomics data in our study was approximately three orders of the magnitude (~1000x), whereas others have reported the shift of 1.3x [21] and ~5x [23]. Several differences between this study and the two above-mentioned studies exist that could have contributed to this disparity. These include differences in cell types (human endothelial cells *vs.* human liver spheroids), exposure durations (6 and 12 weeks *vs.* 10–14 days), and PFOA concentration ranges (nM *vs.* μM), all of which can influence sensitivity of the response. Importantly, the long-term exposure approach, which permitted the use of lower, nanomolar concentrations of PFOA, resulted in significantly lower BMC values. Our

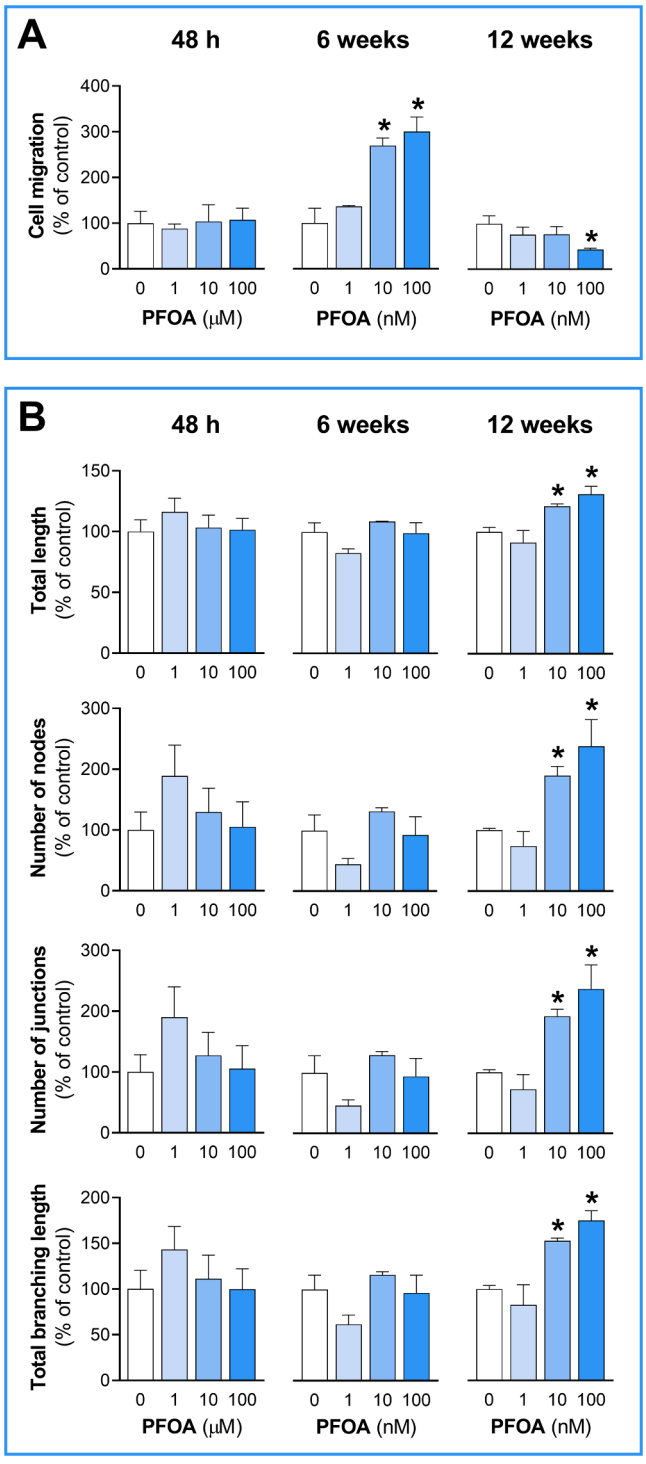

Fig. 4. The effect of short-term and long-term exposure of EA.hy926 cells to PFOA on cell migration and endothelial tube formation. EA.hy926 cells were exposed to 1 μM, 10 μM, and 100 μM PFOA or vehicle (0.05 % DMSO; 0 μM PFOA) for 48 h (short-term exposure) and 1 nM, 10 nM, and 100 nM PFOA or vehicle (0.05 % DMSO; 0 nM PFOA) for 6 and 12 weeks (long-term exposure), followed by the assessment of (A) cell migration using the modified Boyden chamber assay and (B) the extent of angiogenesis *in vitro* using three-dimensional matrix Cultrex Reduced Growth Factor Basement Membrane Extract. The results were expressed relative to the vehicle-treated control (100 %). Each data bar represents the mean ± SEM of 4 independent experiments (short-term exposure) or 3 cell culture flasks (long-term exposure). *$p < 0.05$ *vs.* control.

findings emphasize the critical role of exposure duration in shaping both apical and transcriptomic responses. Although we cannot define a single "optimal" chronic exposure duration, our results indicate that both 6-week and 12-week exposures are biologically relevant and should be considered in future *in vitro* toxicological assessments. This is a critical consideration for downstream HED calculations and risk predictions. It is also important to note that not all data in our study followed classical monotonic dose-response or linear time-effect patterns. Such non-linear responses are not uncommon in studies of PFAS, including PFOA, and are consistent with non-monotonic dose-response (NMDR) behavior that has been previously reported in the literature [34–37]. In our study, several apical and transcriptomic endpoints, including cell migration, monocyte adhesion, and the number of DEGs, exhibited NMDR behavior, with the most pronounced effects occurring at 10 nM PFOA or at the 6-week time point. However, those NMDR responses were filtered out using the Williams Trend Test and only endpoints with monotonic dose-responses were included in our BMC and HED analyses.

4.2. *Potential mode of action of PFOA in human vascular endothelial cells*

The mechanism through which PFOA exerts toxicity in endothelial cells remains poorly understood. Previous research has suggested that PFOA induces vascular network formation *via* the NOTCH signaling pathway in embryonic trophoblast cells [17] and inhibits placental development in mice through apoptosis and structural changes in placental vasculature [19]. Our study provides new insights into how PFOA might affect human vascular endothelial cells. Though endothelial cells are not typically the primary focus of toxicology studies, they represent the initial point of contact for chemicals in the bloodstream, including PFOA. Our findings suggest that short-term exposure to PFOA activates transcription and signaling pathways associated with NTRKs in EA.hy926 cells, while long-term exposure is linked to IL signaling and ECM organization. Some pathways associated with transcription were observed to overlap between exposure durations (e.g., 48 h *vs.* 6 weeks). Our data did not provide a possible link between pathways and apical changes at the 48-h time point due to a lack of dose-dependent responses. On the other hand, IL signaling, transcription, and ECM organization may be linked to the apical changes observed after long-term exposure of EA.hy926 cells to PFOA. IL-10, in particular, is known to play a critical role in angiogenesis [38]. Other interleukins identified in this study, such as IL-7, IL-13, and IL-4, are also known to be involved in angiogenesis [39–41], endothelial cell proliferation [42], and induction of vascular cell adhesion molecule-1 [43]. Additionally, ECM remodeling is closely related to both angiogenesis [44–48] and endothelial permeability [49–51]. Our results reveal that the median BMC values for pathways are in the narrow range of those obtained from apical endpoints suggesting that PFOA may influence endothelial function through these molecular pathways, particularly after prolonged exposure.

4.3. *HED and BER*

In this study, the BMC values were taken as Css in human plasma and used to calculate HED. The lowest HED derived from apical changes (A-HED) was 0.59 ng/kg bw/week following 6 weeks of exposure. After 12 weeks, the median A-HED was 4.32 ng/kg bw/week, while the lower bound 10th percentile HED was 0.59 ng/kg bw/week. However, it is important to note that the A-HED calculated after 6 weeks of exposure is based on a single apical endpoint, introducing some uncertainty. Nonetheless, these values are informative, as they reflect a complex biological response. The lowest transcriptomic HED (T-HED) calculated after 6 weeks of exposure using Approach 1 was a median of 3.6 ng/kg bw/week, with the lower bound 10th percentile HED at 1.25 ng/kg bw/week. Using Approach 2, pathway-level HEDs were slightly higher than gene-level HEDs, ranging from 3.0 ng/kg bw/week for NGF-stimulated transcription to 3.2 ng/kg bw/week for IL-4 and IL-13 signaling. Importantly, both gene- and pathway-level HEDs were below the

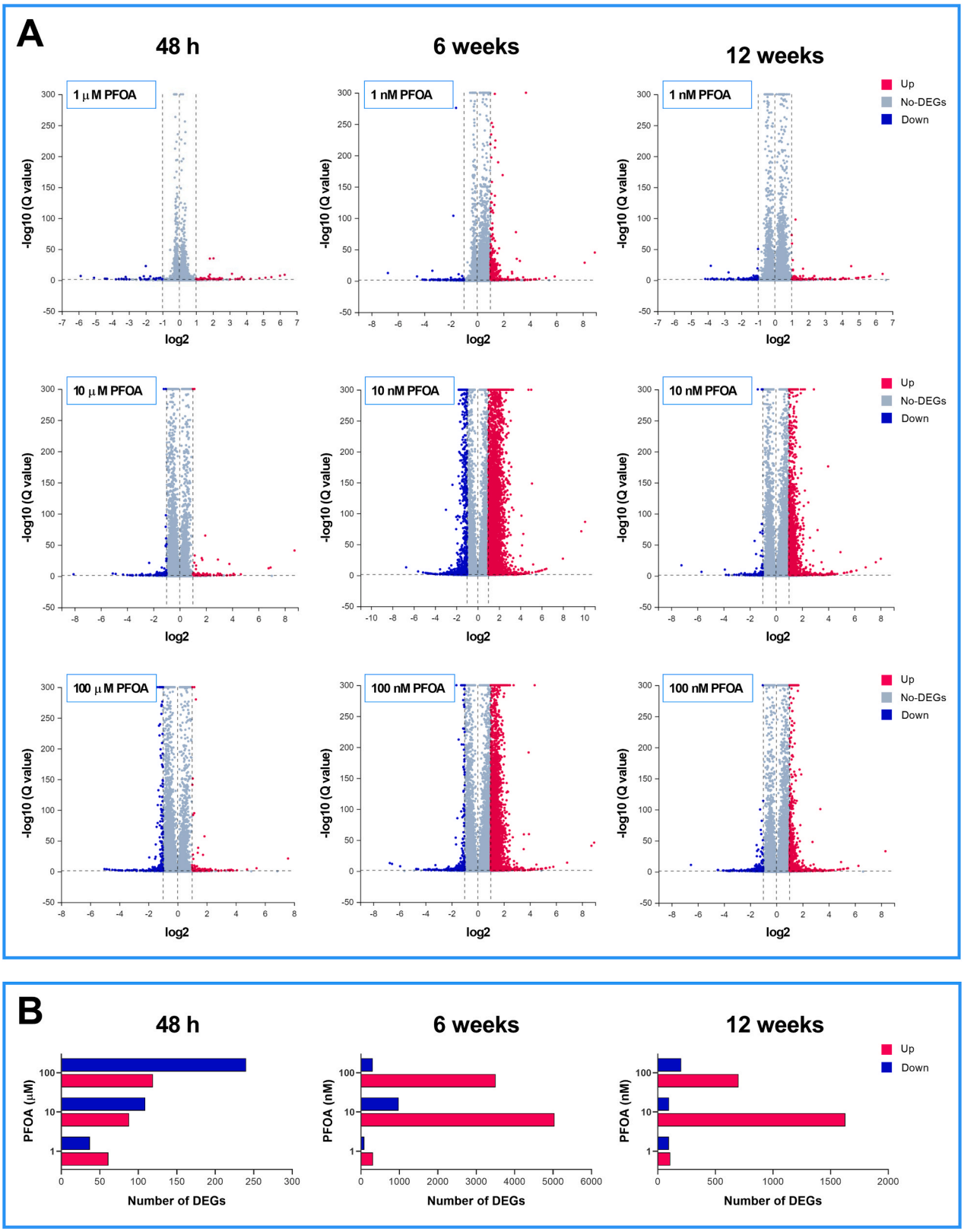

Fig. 5. Volcano scatter plots depicting global mRNA expression and the number of DEGs following short-term (48 h) and long-term (6 and 12 weeks) exposure of EA. hy926 cells to the specified concentrations of PFOA. (A) The X-axis represents the fold change of the difference after conversion to log2, whereas the Y-axis represents the significance value (Q value) after conversion to –log10. In each plot, significantly upregulated genes are marked as red dots, downregulated genes as blue dots, and non-significant findings as gray dots. (B) The X-axis displays the number of DEGs, and the Y-axis shows the different concentrations of PFOA. For each concentration, red bar represents the number of upregulated genes, while blue bar represents the number of downregulated genes.

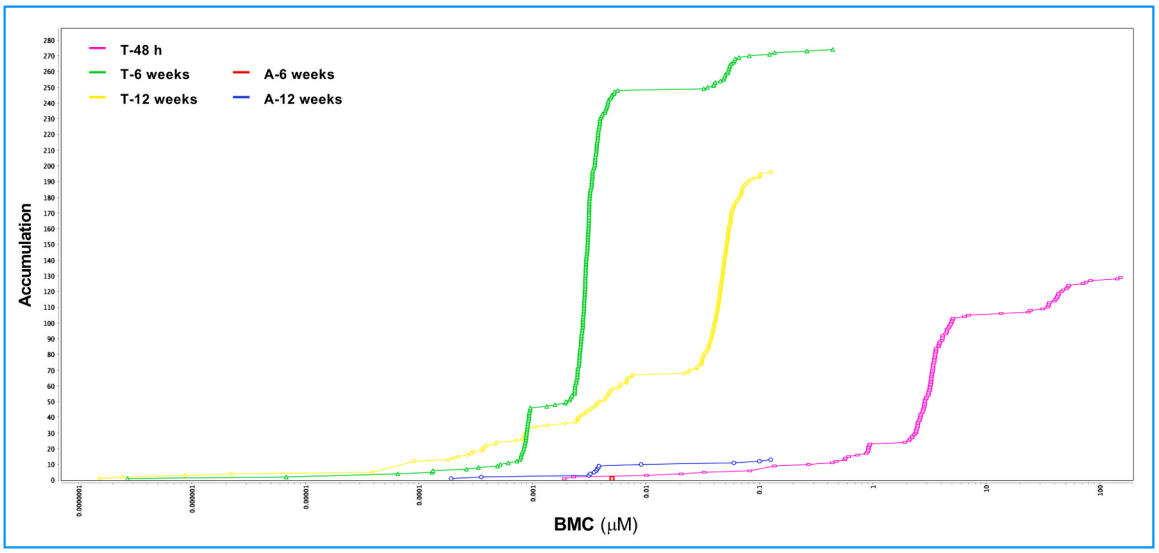

Fig. 6. Accumulation plots of BMC values for apical (A) and transcriptomics (T) data following short-term (48 h) and long-term (6 and 12 weeks) exposure of EA. hy926 cells to PFOA. The analysis was conducted in BMDExpress v3.20.0106.

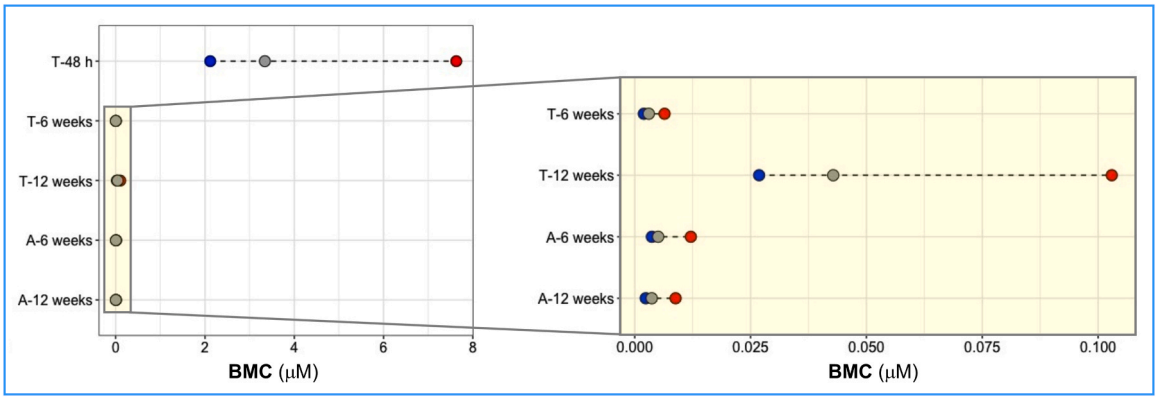

Fig. 7. Range plot of PFOA BMC values. Median lower confidence limit (BMCL; blue dot), median confidence limit (BMC; grey dot), and median upper confidence limit (BMCU; red dot) of the BMC values for apical (A) and transcriptomics (T) data following short-term (48 h) and long-term (6 and 12 weeks) exposure of EA. hy926 cells to PFOA. For improved visualization, the expanded pale-yellow panel on the right shows the median BMCL, BMC, and BMCU values from long-term exposure study.

estimated exposure level of the U.S. general population (9.91 ng/kg bw/week), which means that BER values were less than 1. For BER calculations, we used the 95th percentile of serum PFOA concentrations from the U.S. NHANES data (2017–March 2020), as it reflects the value below which 95 % of measured PFOA levels in the blood serum of a population fall and is commonly used in human health risk assessments to evaluate sensitive subpopulations or individuals with elevated exposure. This approach is consistent with regulatory guidance [26,52] and routinely applied in the scientific literature [20,23,24]. In our study, BER values were lower than those reported by Rowan-Caroll et al., who applied a similar approach using human primary liver cell spheroids [23]. On the other hand, our BERs were comparable to those reported by Fragki et al. in an acute exposure study where HepaRG cells were exposed to micromolar concentrations of PFOA for 24 h. In that study, the calculated oral equivalent effect doses for gene expression were lower than the upper bound chronic dietary exposure estimates [24]. Although these findings suggest that acute *in vitro* exposure can also yield sensitive HED estimates comparable to those from chronic exposures, it is important to consider the role of PBTK model assumptions. Fragki et al. derived HEDs based on a continuous oral exposure scenario over a 50-year period, while our PBTK model estimated HEDs over a significantly shorter exposure duration of 16,000 h. These differences in exposure duration and modeling assumptions highlight the importance of context when interpreting and comparing HED predictions across studies. At the gene level, HED analysis identified several candidates with potential biomarker relevance for endothelial responses to chronic PFOA exposure. *IL1A*, *CXCL8*, and *KLF4* emerged as consistent markers across time points. These genes are known to play critical roles in endothelial physiology, and their derived HED values were within one order of magnitude of the general U.S. population's estimated exposure level. While promising, the potential use of these genes as biomarkers requires further validation through epidemiological and mechanistic studies.

4.4. Sensitivity of different populations to PFOA

The derivation of regulatory safe limit for PFOA or combined PFAS exposure took into consideration exposure levels of different human populations. It has been shown that toddlers and other children have approximately two-fold higher mean intake of PFAS than older age groups [26]. However, the exposure level of other sensitive human populations is currently unknown. The main question we should ask is "Do the most sensitive populations benefit from the current regulation?" [53]. Sensitive populations, such as those suffering from various chronic

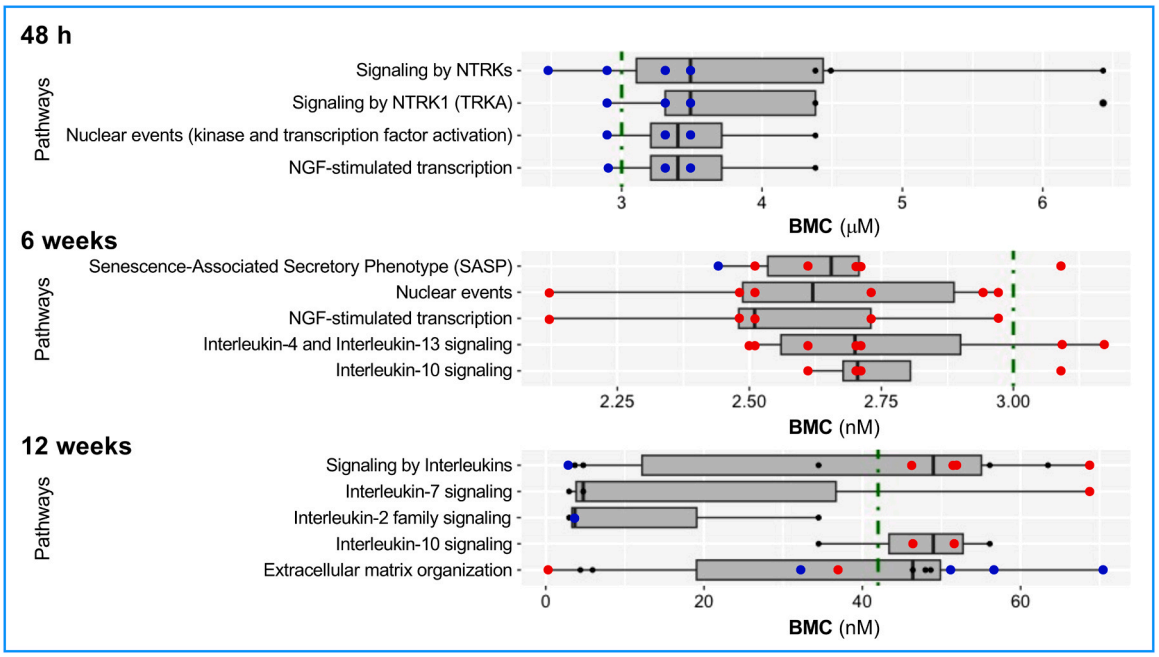

Fig. 8. BMC values of individual genes classified into pathways following short-term (48 h) and long-term (6 and 12 weeks) exposure of EA.hy926 cells to PFOA. The pathway analysis was conducted using Reactome. The grey box represents the range between the 1st and the 3rd quartile, while the solid black line indicates the median BMC value. The green dashed vertical line indicates the median BMC value of all genes at each exposure time point. The upregulated genes are marked as red dots, downregulated genes as blue dots, and unaffected genes as black dots.

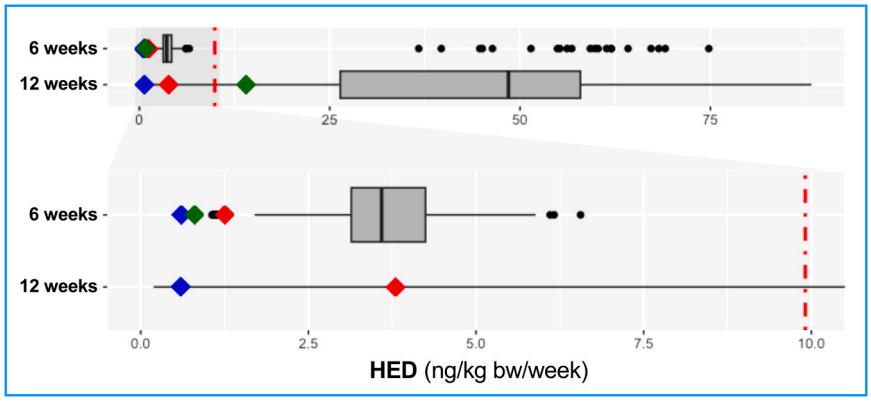

Fig. 9. The boxplot of HED values obtained from transcriptomic data (T) and apical assays (A) in EA.hy926 cells after 6 and 12 weeks of exposure to PFOA. The red diamond indicates the lower bound 10th percentile T-HED, the blue diamond indicates the lower bound 10th percentile A-HED, and the green diamond indicates the median HED of the genes from the most sensitive pathway. The grey box represents the range between the 1st and the 3rd quartile, while the solid black line indicates the median HED value. The red dashed line indicates an estimated weekly exposure to PFOA of the U.S. general population.

Table 3
Calculated BERs based on predicted HEDs.

	Approach 1			Approach 2			
Population exposure (ng/kg bw/week)	**HED** (ng/kg bw/week)		**BER**	**HED** (ng/kg bw/week)		**Pathway**	**BER**
9.91[#]	T−6 weeks	1.25	0.12	T−6 weeks	3.0	NGF-stimulated transcription	0.30
	T−12 weeks	3.84	0.39	T−12 weeks	55.0	Interleukin−10 signaling	5.55
	A−6 weeks	0.59*	0.06	A−6 weeks	/	/	/
	A−12 weeks	0.59	0.06	A−12 weeks	/	/	/

– calculated from the 95th percentile of serum PFOA concentration obtained from the U.S. NHANES (2017–March 2020) and reported in the paper by Botelho et al. (2025)
* – obtained from one HED value

Table 4
HED and BER values for transcriptomic biomarkers of endothelial function following long-term exposure of EA.hy926 cells to PFOA.

Gene	Biological processes[#]	HED (ng/kg bw/week)		BER*	
		6 weeks	12 weeks	6 weeks	12 weeks
IL1A	Inflammatory response; Positive regulation of angiogenesis; Positive regulation of vascular endothelial growth factor production; Positive regulation of cytokine production	3.13	52.47	0.32	5.29
CXCL8	Angiogenesis; Positive regulation of angiogenesis; Induction of positive chemotaxis; Inflammatory response; Negative regulation of cell adhesion molecule production; Regulation of cell adhesion	3.23	58.38	0.33	5.89
KLF4	Cellular response to laminar fluid shear stress; Negative regulation of angiogenesis; Negative regulation of cell migration involved in sprouting angiogenesis; Negative regulation of inflammatory response; Negative regulation of interleukin−8 production; Negative regulation of response to cytokine stimulus; Negative regulation of leukocyte adhesion to arterial endothelial cell; Positive regulation of nitric oxide biosynthetic process; Positive regulation of sprouting angiogenesis	3.33	6.64	0.34	0.67

– GO terms obtained from UniProt (https://www.uniprot.org/)
* – calculated as the ratio between HED and estimated exposure of the U.S. general population (9.91 ng/kg bw/week)

diseases, may have a different PFOA toxicokinetics affecting the level of this compound in the plasma and its bioactive concentrations. It has been shown that the decreased expression of transporters, such as OAT-3, OAT-4, and GFR, results in higher PFOA concentrations in the plasma of exposed rats than in the group of healthy animals with normal expression of the aforementioned transporters [54]. These data clearly indicate that the toxicokinetics of PFOA was affected by alterations in kidney function, which can limit the effectiveness of risk assessment and prevent identification of populations particularly vulnerable to PFOA exposure. Bearing this in mind, we estimated exposure to PFOA in several sensitive population subgroups based on the BMC values calculated from long-term exposure of endothelial cells. Our study predicts that individuals with impaired renal function, liver disease or obesity have lower HEDs, meaning that they could reach bioactive concentrations of PFOA at lower exposure. For example, individuals with ESRD or moderate to severe GFR reduction may reach a threshold for endothelial dysfunction at much lower PFOA concentrations compared to healthy individuals. To be specific, our analysis shows that individuals suffering from ESRD, moderate to severe decrease in GFR, cirrhosis CP class A, NAFLD, and obesity class 1 have a lower average 10th percentile HED than the healthy adult population. Those individuals are at higher risk of activating the NGF-stimulated transcription pathway, which has been identified as the most sensitive pathway contributing to endothelial dysfunction due to PFOA exposure. Interestingly, not all examined population subgroups in this study showed increased risk of PFOA exposure. Our analysis has shown that the individuals with mild decrease in GFR, cirrhosis CP class B and C, and simple steatosis have estimated HED values above those calculated for the healthy adult population. This finding suggests that a set of specific health parameters for each disease impacts the toxicokinetics of PFOA, thereby affecting the estimated HEDs. Currently, it is difficult to provide an explanation for the observed difference in the estimated HEDs between these population subgroups. It has been shown that rats with alterations in GFR have a longer PFOA half-life compared to normal rats leading to higher levels of this compound in plasma [54]. We noticed the same effect in our study – the same level of exposure (~2 mg PFOA/kg bw/week) leads to the Css value of 0.87 ng PFOA/mL plasma in individuals with ESRD and 1.0 ng PFOA/mL plasma in those with a moderate decrease in GFR. At the same time, the Css value in a healthy adult population is predicted to be 0.65 ng PFOA/mL plasma. It can be assumed that the toxicokinetics of PFOA in individuals with moderate to severe decrease in GFR results in longer PFOA half-life, thereby lowering the estimated HED. On the other hand, a mild decrease in GFR shows an opposite effect on the estimated HED and the bioactive PFOA level than the other forms of GFR impairment; however, the reason for this discrepancy is not known. A similar effect was predicted in population subgroups with different levels of hepatic impairment – an opposite effect on estimated HEDs was predicted in individuals with different stages of cirrhosis and those affected by NAFLD. This finding is somewhat expected, considering that it has been shown that different types of liver dysfunction can affect the pharmacokinetics of drugs [55–57]. For example, our analysis has shown lower HEDs in a population subgroup with mild liver disease (cirrhosis CP class A) compared to the healthy population, whereas the opposite effect has been predicted in individuals with later stages of cirrhosis (CP classes B and C). A similar effect was also predicted for population subgroups with different stages of NAFLD. While increased HED values were predicted for individuals with simple steatosis compared to a healthy population, decreased values were predicted for the population with NAFLD. These results suggest that individuals with cirrhosis CP class A and NAFLD can reach plasma bioactive concentration with lower exposure to PFOA than those affected by later stages of cirrhosis (CP classes B and C) or simple steatosis. Of particular interest is the predicted HED in a population with obesity class 1. Our analysis has predicted substantially lower HED in this population subgroup – down to ~40 % of the HED in a healthy population. Based on the predicted HED, we can argue that obesity class 1 substantially increases the risk of PFOA-induced endothelial effects, as these individuals are predicted to have a higher bioactive concentration of PFOA in their plasma compared to the general population. This finding is expected, considering that obesity affects many physiological parameters, including the pharmacokinetics of drugs [58]. The predicted increased risk of PFOA exposure in individuals with class 1 obesity is particularly concerning given global obesity trends. According to the World Health Organization (WHO), 16 % of adults worldwide were classified as obese in recent years, with the global prevalence of obesity more than doubling between 1990 and 2022 (WHO Fact sheets_Obesity and overweight). Projections from the World Obesity Atlas suggest that by 2030, approximately 26 % of adults (around 745 million) may be living with class 1 obesity (World Obesity Atlas). When considering the additional prevalence of other chronic conditions investigated in this study such as NAFLD, with an estimated global prevalence of 30.2 % [59], a substantial portion of the global population could face heightened vulnerability to PFOA exposure.

4.5. *Limitations of the study*

We acknowledge several limitations in this study. The use of the EA.hy926 human macrovascular endothelial cell line, which is immortalized and transformed, may not fully replicate the responses of primary or native human endothelial cells. However, this cell line enabled us to conduct the long-term exposure study, which would be technically challenging with primary cells due to their limited lifespan. EA.hy926

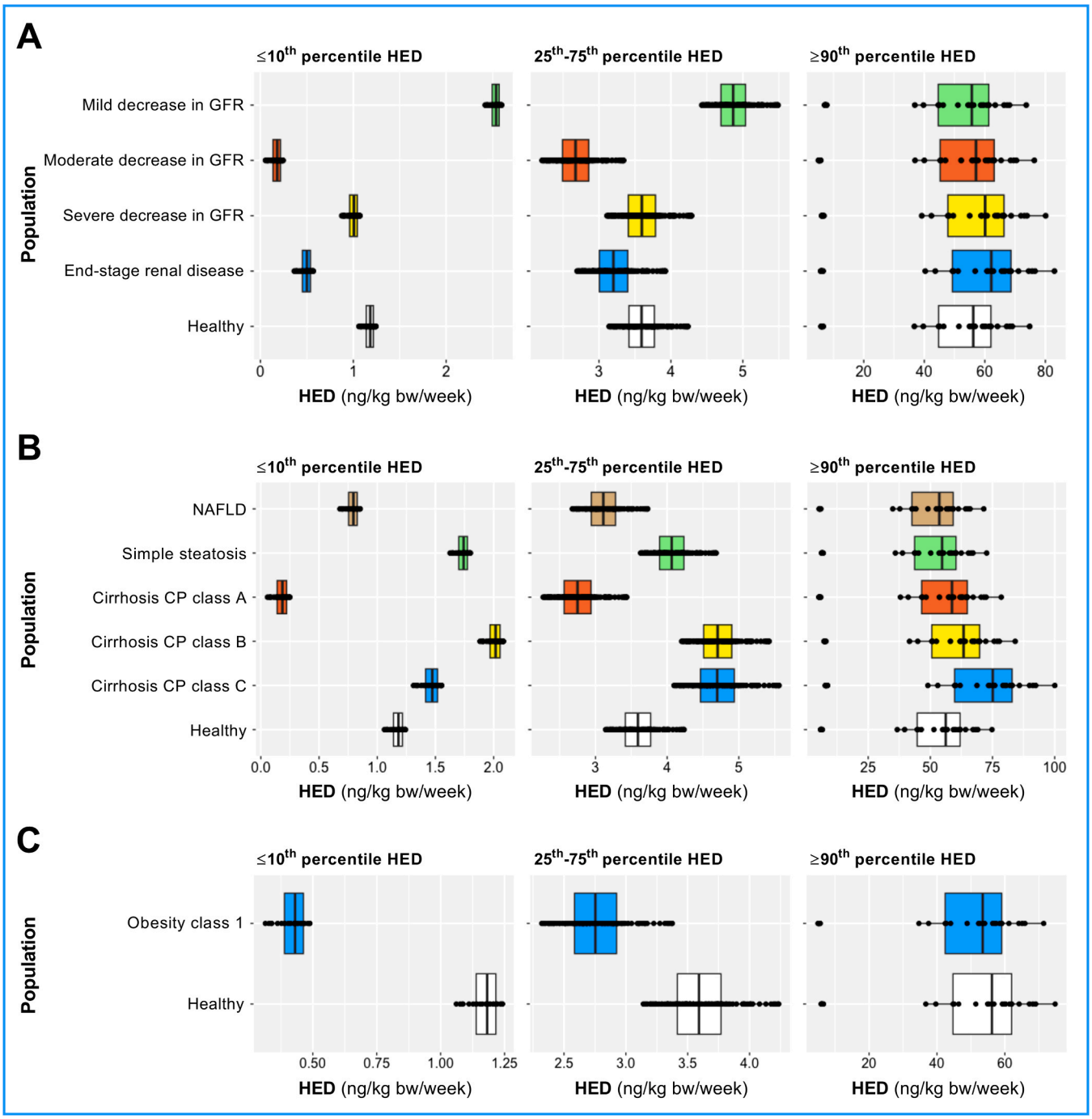

Fig. 10. The boxplot of HED values for different human populations obtained after 6-week exposure of EA.hy926 cells to PFOA. The comparison between healthy adult population and (A) adult population with different stages of renal impairment, (B) adult population with different stages of liver disease, and (C) obese adult population is shown. The white box represents the range between the 1st and the 3rd quartile of the healthy population, while the colored boxes represent the range between the 1st and the 3rd quartile of the populations with different diseases. The solid black line indicates the median HED value.

cells provided a robust system for mechanistic and high-resolution analysis of molecular and cellular responses, including transcriptomic profiling, under tightly controlled exposure conditions, which was essential for our study design. While the *in vitro* model offers valuable insights, it cannot fully reproduce the complexity of *in vivo* systems, including multicellular interactions, extracellular matrix dynamics, and systemic feedback. To help bridge this gap, we used chronic low-dose exposure scenarios with environmentally relevant concentrations of PFOA (1, 10, and 100 nM) and extended the exposure duration up to 12 weeks. By doing so, we have partially eliminated the issue of exposure duration, which is usually several hours to a few days in the majority of *in vitro* assays *vs.* weeks, months or years in *in vivo* studies. Nevertheless, while the 12-week exposure duration in our study was designed to mitigate short-term exposure limitations, challenges related to replicating the complexity of living organisms remain. We would like to highlight a lack of published *in vivo* studies investigating the effects of PFOA on endothelial cells that we could use to strengthen our *in vitro* findings. However, ongoing *in vivo* studies in our laboratory will further validate and expand upon the findings presented here. These future results will help contextualize the apical and transcriptomic outcomes in

Table 5
The median HED values (ng/kg bw/week) with 95 % confidence intervals (CI) for different populations calculated using different ranges of Css[#].

Population	≤ 10th percentile Css	25th–75th percentile Css	≥ 90th percentile Css
Healthy	1.18 (CI: 1.16–1.20)	3.59 (CI: 3.54–3.64)	56.18 (CI: 47.93–64.44)
End-stage liver disease	**0.50*** (CI: 0.48–0.52)	**3.20*** (CI: 3.15–3.25)	62.13 (CI: 52.88–71.38)
Severe decrease in GFR	**1.00*** (CI: 0.98–1.03)	3.59 (CI: 3.54–3.65)	60.09 (CI: 51.22–68.96)
Moderate decrease in GFR	**0.18*** (CI: 0.16–0.20)	**2.67*** (CI: 2.62–2.72)	57.09 (CI: 48.55–65.63)
Mild decrease in GFR	**2.54*** (CI: 2.52–2.56)	**4.87*** (CI: 4.82–4.91)	55.69 (CI: 47.71–63.67)
Cirrhosis CP class A	**0.18*** (CI: 0.16–0.21)	**2.75*** (CI: 2.70–2.80)	58.70 (CI: 49.92–67.49)
Cirrhosis CP class B	**2.02*** (CI: 1.99–2.04)	**4.70*** (CI: 4.65–4.76)	63.36 (CI: 54.15–72.57)
Cirrhosis CP class C	**1.47*** (CI: 1.44–1.50)	**4.70*** (CI: 4.63–4.76)	**75.11*** (CI: 64.06–86.16)
Simple steatosis	**1.74*** (CI: 1.72–1.76)	**4.06*** (CI: 4.02–4.11)	54.72 (CI: 46.77–62.67)
NAFLD	**0.79*** (CI: 0.77–0.82)	**3.11*** (CI: 3.06–3.15)	53.61 (CI: 45.68–61.54)
Obesity class 1	**0.43*** (CI: 0.41–0.45)	**2.75*** (CI: 2.71–2.80)	53.47 (CI: 45.51–61.43)

[#] – bioactive PFOA concentration obtained after 6-week exposure of EA.hy926 cells
* – statistical significance compared to the healthy adult population

a whole-organism setting. We also recognize that the translation of *in vitro* effects to *in vivo* outcomes introduces uncertainty. The changes in gene expression or apical endpoints observed here may not directly correspond to equivalent biological effects in animals or humans. For instance, the BER in this study was derived from the lower bound 10th percentile HED, representing a 10 % change from the control. However, whether a 10 % change in gene expression *in vitro* corresponds to a similar biological effect *in vivo* remains uncertain. Another important consideration involves serum protein binding. Albumin concentrations in *in vitro* assays differ significantly from those *in vivo*. It has been shown that the free fraction of PFOA, which represents its bioactive concentration, can vary by up to two orders of magnitude, depending on albumin levels [60], potentially impacting the interpretation of cellular responses. In terms of modeling, our PBTK simulations were limited to a two-year timeframe, due to model complexity and the large number of input parameters required. While this timeframe captures critical exposure windows, longer simulations may be necessary for evaluating life-span or developmental impacts. Moreover, we acknowledge that the PFOA concentration range used in this study may appear limited for deriving robust BMC values. Although BMD guidance [61] does not explicitly state a minimum number of dose groups, incorporating additional concentrations would enhance the robustness of the BMC and HED estimates. We opted to use three biologically relevant PFOA concentrations (1, 10, and 100 nM) in addition to the control based on several considerations. First, long-term *in vitro* experiments spanning up to 12 weeks, such as those conducted in this study, are inherently resource- and time-intensive, and introduce challenges in maintaining stable conditions across multiple replicates and endpoints. Second, the concentration range selected was based on previous studies and human biomonitoring data, aiming to reflect environmentally relevant exposure levels, especially around or below the 95th percentile of serum PFOA concentrations in the general population. Third, although the number of dose groups was limited, the concentrations used covered three orders of magnitude and the sufficient amount of data showed a clear dose-response trend, enabling the derivation of meaningful BMC values with acceptable model fit. However, future studies should aim to include additional concentration groups to strengthen dose-response modeling. Finally, while we acknowledge that direct experimental validation of our population-specific predictions is currently limited by the lack of toxicokinetic or biomonitoring data in humans with liver or kidney impairment or obesity, our model provides a testable framework for future studies – individuals with renal or hepatic impairment or obesity will exhibit earlier or stronger endothelial responses to PFOA exposure. Future clinical biomonitoring studies and *in vivo* toxicokinetic modeling in these population groups could empirically validate our predictions.

5. Conclusions

This study advances the application of an *in vitro*-PBTK modeling approach as an alternative method for human health risk assessment of environmental chemicals, using PFOA as a case study. Our findings indicate that the predicted HEDs, derived from both apical and transcriptomic data, are lower than estimated exposure level for the U.S. general population. These findings raise important concerns regarding the potential health risks associated with dietary exposure to PFOA. Furthermore, our analysis suggests that certain sensitive populations, including individuals with ESRD, moderate to severe decrease in GFR, cirrhosis CP class A, NAFLD, and class 1 obesity, may be at greater risk of endothelial dysfunction resulting from PFOA exposure. Given the global prevalence of these conditions, the data presented here may support the need for a reassessment of current regulatory safety thresholds for PFOA. In conclusion, this study demonstrates the potential of integrating long-term low-level *in vitro* studies using human cells and *in silico* methodologies coupled with population-specific analyses within risk assessment frameworks to better evaluate the health impact of environmental chemicals. Such approaches offer a powerful tool for screening a large number of substances, especially in cases where traditional toxicity data are limited.

Environmental implication

Our study reveals that long-term low-level exposure to PFOA induces sensitive biological responses in human vascular endothelial cells at doses below current exposure levels observed in the U.S. general population. Certain groups, including individuals with obesity and those with liver or kidney impairments show heightened sensitivity, suggesting a substantial portion of the global population may be at increased risk. These findings emphasize the need to reassess current regulatory safety thresholds for PFOA and highlight the importance of incorporating data obtained from long-term low-level *in vitro* studies into regulatory risk assessments to better protect public health and guide environmental policies.

CRediT authorship contribution statement

Marija Opacic: Writing – review & editing, Writing – original draft, Methodology, Investigation, Formal analysis. **Nemanja Todorovic:** Writing – review & editing, Writing – original draft, Software, Methodology, Formal analysis. **Mladena Lalic-Popovic:** Writing – review & editing, Writing – original draft, Software, Methodology, Formal analysis. **Bojana Stanic:** Writing – review & editing, Writing – original draft, Visualization, Supervision, Methodology, Investigation, Formal analysis, Conceptualization. **Nebojsa Andric:** Writing – review & editing, Writing – original draft, Visualization, Supervision, Funding acquisition, Formal analysis, Conceptualization.

Funding

This research was supported by the Science Fund of the Republic of Serbia, Grant No. 7010, "Integration of Biological Responses and PBTK Modeling in Chemical Toxicity Assessment: A Case Study of Perfluorooctanoic Acid (PFOA) – ToxIN".

Declaration of Competing Interest

The authors declare that they have no known competing financial interests or personal relationships that could have appeared to influence the work reported in this paper.

Acknowledgements

The authors are grateful to Branko Sikoparija and Jelena Jovic (BioSense Institute, Novi Sad, Serbia) for their help in using Amnis® ImageStream®X Mk II Imaging Flow Cytometry instrument.

Appendix A. Supporting information

Supplementary data associated with this article can be found in the online version at doi:10.1016/j.jhazmat.2025.139402.

Data availability

Data will be made available on request.

References

[1] Wee, S.Y., Aris, A.Z., 2023. Environmental impacts, exposure pathways, and health effects of PFOA and PFOS. Ecotoxicol Environ Saf 267, 115663. https://doi.org/10.1016/j.ecoenv.2023.115663.

[2] Land, M., de Wit, C.A., Bignert, A., Cousins, I.T., Herzke, D., Johansson, J.H., et al., 2018. What is the effect of phasing out long-chain per- and polyfluoroalkyl substances on the concentrations of perfluoroalkyl acids and their precursors in the environment? A systematic review. Environ Evid 7 (1), 4. https://doi.org/10.1186/s13750-017-0114-y.

[3] Botelho, J.C., Kato, K., Wong, L.Y., Calafat, A.M., 2025. Per- and polyfluoroalkyl substances (PFAS) exposure in the U.S. Population: NHANES 1999-March 2020. Environ Res 270, 120916. https://doi.org/10.1016/j.envres.2025.120916.

[4] Batzella, E., Rosato, I., Pitter, G., Da Re, F., Russo, F., Canova, C., et al., 2024. Determinants of PFOA serum Half-Life after end of exposure: a longitudinal study on highly exposed subjects in the veneto region. Environ Health Perspect 132 (2), 27002. https://doi.org/10.1289/EHP13152.

[5] Pitter, G., Da Re, F., Canova, C., Barbieri, G., Zare Jeddi, M., Dapra, F., et al., 2020. Serum levels of perfluoroalkyl substances (PFAS) in adolescents and young adults exposed to contaminated drinking water in the veneto region, Italy: a Cross-Sectional study based on a health surveillance program. Environ Health Perspect 128 (2), 27007. https://doi.org/10.1289/EHP5337.

[6] Steenland, K., Tinker, S., Frisbee, S., Ducatman, A., Vaccarino, V., 2009. Association of perfluorooctanoic acid and perfluorooctane sulfonate with serum lipids among adults living near a chemical plant. Am J Epidemiol 170 (10), 1268–1278. https://doi.org/10.1093/aje/kwp279.

[7] Li, K., Gao, P., Xiang, P., Zhang, X., Cui, X., Ma, L.Q., 2017. Molecular mechanisms of PFOA-induced toxicity in animals and humans: implications for health risks. Environ Int 99, 43–54. https://doi.org/10.1016/j.envint.2016.11.014.

[8] White, S.S., Fenton, S.E., Hines, E.P., 2011. Endocrine disrupting properties of perfluorooctanoic acid. J Steroid Biochem Mol Biol 127 (1-2), 16–26. https://doi.org/10.1016/j.jsbmb.2011.03.011.

[9] Krüger-Genge, A., Blocki, A., Franke, R.P., Jung, F., 2019. Vascular endothelial cell biology: an update. Int J Mol Sci 20 (18), 4411. https://doi.org/10.3390/ijms20184411.

[10] Kokai, D., Markovic Filipovic, J., Opacic, M., Ivelja, I., Banjac, V., Stanic, B., et al., 2024. *in vitro* and *in vivo* exposure of endothelial cells to dibutyl phthalate promotes monocyte adhesion. Food Chem Toxicol 188, 114663. https://doi.org/10.1016/j.fct.2024.114663.

[11] Kokai, D., Stanic, B., Samardzija Nenadov, D., Pogrmic-Majkic, K., Tesic, B., Fa, S., et al., 2020. Biological effects of chronic and acute exposure of human endothelial cell line EA.hy926 to bisphenol A: new tricks from an old dog. Chemosphere 256, 127159. https://doi.org/10.1016/j.chemosphere.2020.127159.

[12] Kokai, D., Stanic, B., Tesic, B., Samardzija Nenadov, D., Pogrmic-Majkic, K., Fa Nedeljkovic, S., et al., 2022. Dibutyl phthalate promotes angiogenesis in EA.hy926 cells through estrogen receptor-dependent activation of ERK1/2, PI3K-Akt, and NO signaling pathways. Chem Biol Inter 366, 110174. https://doi.org/10.1016/j.cbi.2022.110174.

[13] Stanic, B., Kokai, D., Markovic Filipovic, J., Samardzija Nenadov, D., Pogrmic-Majkic, K., Andric, N., 2023. Global gene expression analysis reveals novel transcription factors associated with long-term low-level exposure of EA.hy926 human endothelial cells to bisphenol a. Chem Biol Inter 381, 110571. https://doi.org/10.1016/j.cbi.2023.110571.

[14] Stanic, B., Kokai, D., Markovic Filipovic, J., Tomanic, T., Vukcevic, J., Stojkov, V., et al., 2024. Vascular endothelial effects of dibutyl phthalate: *in vitro* and *in vivo* evidence. Chem Biol Inter 399, 111120. https://doi.org/10.1016/j.cbi.2024.111120.

[15] Stanic, B., Kokai, D., Tesic, B., Fa, S., Samardzija Nenadov, D., Pogrmic-Majkic, K., et al., 2022. Integration of data from the *in vitro* long-term exposure study on human endothelial cells and the *in silico* analysis: a case of dibutyl phthalate-induced vascular dysfunction. Toxicol Lett 356, 64–74. https://doi.org/10.1016/j.toxlet.2021.12.006.

[16] Kong, Y., Wen, Y., Cao, G., Xu, Y., Zhang, C., Tan, G.C., et al., 2022. Di-n-butyl phthalate promotes monocyte recruitment via miR-137-3p-SP1-MCP-1 pathway. Ecotoxicol Environ Saf 236, 113491. https://doi.org/10.1016/j.ecoenv.2022.113491.

[17] Poteser, M., Hutter, H.P., Moshammer, H., Weitensfelder, L., 2020. Perfluorooctanoic acid (PFOA) enhances NOTCH-signaling in an angiogenesis model of placental trophoblast cells. Int J Hyg Environ Health 229, 113566. https://doi.org/10.1016/j.ijheh.2020.113566.

[18] Liu, Q.S., Hao, F., Sun, Z., Long, Y., Zhou, Q., Jiang, G., 2018. Perfluorohexadecanoic acid increases paracellular permeability in endothelial cells through the activation of plasma kallikrein-kinin system. Chemosphere 190, 191–200. https://doi.org/10.1016/j.chemosphere.2017.10.002.

[19] Jiang, W., Deng, Y., Song, Z., Xie, Y., Gong, L., Chen, Y., et al., 2020. Gestational perfluorooctanoic acid exposure inhibits placental development by dysregulation of labyrinth vessels and uNK cells and apoptosis in mice. Front Physiol 11, 51. https://doi.org/10.3389/fphys.2020.00051.

[20] Gannon, A.M., Moreau, M., Farmahin, R., Thomas, R.S., Barton-Maclaren, T.S., Nong, A., et al., 2019. Hexabromocyclododecane (HBCD): a case study applying tiered testing for human health risk assessment. Food Chem Toxicol 131, 110581. https://doi.org/10.1016/j.fct.2019.110581.

[21] Addicks, G.C., Rowan-Carroll, A., Reardon, A.J.F., Leingartner, K., Williams, A., Meier, M.J., et al., 2023. Per- and polyfluoroalkyl substances (PFAS) in mixtures show additive effects on transcriptomic points of departure in human liver spheroids. Toxicol Sci 194 (1), 38–52. https://doi.org/10.1093/toxsci/kfad044.

[22] Reardon, A.J.F., Rowan-Carroll, A., Ferguson, S.S., Leingartner, K., Gagne, R., Kuo, B., et al., 2021. Potency ranking of Per- and polyfluoroalkyl substances using High-Throughput transcriptomic analysis of human liver spheroids. Toxicol Sci 184 (1), 154–169. https://doi.org/10.1093/toxsci/kfab102.

[23] Rowan-Carroll, A., Reardon, A., Leingartner, K., Gagne, R., Williams, A., Meier, M. J., et al., 2021. High-Throughput transcriptomic analysis of human primary hepatocyte spheroids exposed to Per- and polyfluoroalkyl substances as a platform for relative potency characterization. Toxicol Sci 181 (2), 199–214. https://doi.org/10.1093/toxsci/kfab039.

[24] Fragki, S., Louisse, J., Bokkers, B., Luijten, M., Peijnenburg, A., Rijkers, D., et al., 2023. New approach methodologies: a quantitative *in vitro* to *in vivo* extrapolation case study with PFASs. Food Chem Toxicol 172, 113559. https://doi.org/10.1016/j.fct.2022.113559.

[25] Knutsen, H.K., Alexander, J., Barregård, L., Bignami, M., Brüschweiler, B., Ceccatelli, S., et al., 2018. Risk to human health related to the presence of perfluorooctane sulfonic acid and perfluorooctanoic acid in food. EFSA J 16 (12), e05194. https://doi.org/10.2903/j.efsa.2018.5194.

[26] Schrenk, D., Bignami, M., Bodin, L., Chipman, J.K., Del Mazo, J., Grasl-Kraupp, B., et al., 2020. Risk to human health related to the presence of perfluoroalkyl substances in food. EFSA J 18 (9), e06223. https://doi.org/10.2903/j.efsa.2020.6223.

[27] Love, M.I., Huber, W., Anders, S., 2014. Moderated estimation of fold change and dispersion for RNA-seq data with DESeq2. Genome Biol 15 (12), 550. https://doi.org/10.1186/s13059-014-0550-8.

[28] Yang, L., Allen, B.C., Thomas, R.S., 2007. BMDExpress: a software tool for the benchmark dose analyses of genomic data. BMC Genom 8, 387. https://doi.org/10.1186/1471-2164-8-387.

[29] Fàbrega, F., Kumar, V., Schuhmacher, M., Domingo, J.L., Nadal, M., 2014. PBPK modeling for PFOS and PFOA: validation with human experimental data. Toxicol Lett 230 (2), 244–251. https://doi.org/10.1016/j.toxlet.2014.01.007.

[30] Loccisano, A.E., Campbell Jr., J.L., Andersen, M.E., Clewell 3rd, H.J., 2011. Evaluation and prediction of pharmacokinetics of PFOA and PFOS in the monkey and human using a PBPK model. Regul Toxicol Pharm 59 (1), 157–175. https://doi.org/10.1016/j.yrtph.2010.12.004.

[31] Loccisano, A.E., Longnecker, M.P., Campbell Jr., J.L., Andersen, M.E., Clewell 3rd, H.J., 2013. Development of PBPK models for PFOA and PFOS for human pregnancy and lactation life stages. J Toxicol Environ Health A 76 (1), 25–57. https://doi.org/10.1080/15287394.2012.722523.

[32] Elcombe, C.R., Wolf, C.R., Weswood, A.L., 2011. US Pat Appl Publ US 2013/0029928. Available from: ⟨https://patentimagesstoragegoogleapiscom/24/ee/73/f58267c7d70dde/WO2011101643A1pdf⟩.

[33] Dourson, M., Gadagbui, B., 2021. The dilemma of perfluorooctanoate (PFOA) human half-life. Regul Toxicol Pharm 126, 105025. https://doi.org/10.1016/j.yrtph.2021.105025.

[34] Lauritzen, H.B., Larose, T.L., Oien, T., Sandanger, T.M., Odland, J.O., van de Bor, M., et al., 2018. Prenatal exposure to persistent organic pollutants and child overweight/obesity at 5-year follow-up: a prospective cohort study. Environ Health 17 (1), 9. https://doi.org/10.1186/s12940-017-0338-x.

[35] Mancini, F.R., Rajaobelina, K., Praud, D., Dow, C., Antignac, J.P., Kvaskoff, M., et al., 2018. Nonlinear associations between dietary exposures to perfluorooctanoic acid (PFOA) or perfluorooctane sulfonate (PFOS) and type 2 diabetes risk in women: findings from the E3N cohort study. Int J Hyg Environ Health 221 (7), 1054–1060. https://doi.org/10.1016/j.ijheh.2018.07.007.

[36] Park, S.K., Ding, N., Han, D., 2021. Perfluoroalkyl substances and cognitive function in older adults: should we consider non-monotonic dose-responses and chronic kidney disease? Environ Res 192, 110346. https://doi.org/10.1016/j.envres.2020.110346.

[37] Zheng, X., Pan, Y., Qu, Y., Ji, S., Wang, J., Li, Z., et al., 2024. Associations of serum Per- and polyfluoroalkyl substances with hyperuricemia in adults: a nationwide Cross-Sectional study. Environ Sci Technol 58 (29), 12875–12887. https://doi.org/10.1021/acs.est.3c11095.
[38] Fan, Y., Zhang, W., Huang, X., Fan, M., Shi, C., Zhao, L., et al., 2024. Senescent-like macrophages mediate angiogenesis for endplate sclerosis via IL-10 secretion in Male mice. Nat Commun 15 (1), 2939. https://doi.org/10.1038/s41467-024-47317-1.
[39] Gao, R., Zhou, P., Li, Y., Li, Q., 2023. High glucose-induced IL-7/IL-7R upregulation of dermal fibroblasts inhibits angiogenesis in a paracrine way in delayed diabetic wound healing. J Cell Commun Signal 17 (3), 1023–1038. https://doi.org/10.1007/s12079-023-00754-x.
[40] Hong, K.H., Cho, M.L., Min, S.Y., Shin, Y.J., Yoo, S.A., Choi, J.J., et al., 2007. Effect of interleukin-4 on vascular endothelial growth factor production in rheumatoid synovial fibroblasts. Clin Exp Immunol 147 (3), 573–579. https://doi.org/10.1111/j.1365-2249.2006.03295.x.
[41] Peluzzo, A.M., Autieri, M.V., 2022. Challenging the paradigm: Anti-Inflammatory interleukins and angiogenesis. Cells 11 (3), 587. https://doi.org/10.3390/cells11030587.
[42] Lee, I.Y., Kim, J., Ko, E.M., Jeoung, E.J., Kwon, Y.G., Choe, J., 2002. Interleukin-4 inhibits the vascular endothelial growth factor- and basic fibroblast growth factor-induced angiogenesis *in vitro*. Mol Cells 14 (1), 115–121. https://doi.org/10.1016/S1016-8478(23)15081-3.
[43] Schnyder, B., Lugli, S., Feng, N., Etter, H., Lutz, R.A., Ryffel, B., et al., 1996. Interleukin-4 (IL-4) and IL-13 bind to a shared heterodimeric complex on endothelial cells mediating vascular cell adhesion molecule-1 induction in the absence of the common gamma chain. Blood 87 (10), 4286–4295. https://doi.org/10.1182/blood.V87.10.4286.bloodjournal87104286.
[44] Davis, G.E., Kemp, S.S., 2023. Extracellular matrix regulation of vascular morphogenesis, maturation, and stabilization. Cold Spring Harb Perspect Med 13 (4). https://doi.org/10.1101/cshperspect.a041156.
[45] Geindreau, M., Bruchard, M., Vegran, F., 2022. Role of cytokines and chemokines in angiogenesis in a tumor context. Cancers 14 (10), 2446. https://doi.org/10.3390/cancers14102446.
[46] Mongiat, M., Andreuzzi, E., Tarticchio, G., Paulitti, A., 2016. Extracellular matrix, a hard player in angiogenesis. Int J Mol Sci 17 (11), 1822. https://doi.org/10.3390/ijms17111822.
[47] Neve, A., Cantatore, F.P., Maruotti, N., Corrado, A., Ribatti, D., 2014. Extracellular matrix modulates angiogenesis in physiological and pathological conditions. Biomed Res Int 2014, 756078. https://doi.org/10.1155/2014/756078.
[48] Wang, D., Brady, T., Santhanam, L., Gerecht, S., 2023. The extracellular matrix mechanics in the vasculature. Nat Cardiovasc Res 2 (8), 718–732. https://doi.org/10.1038/s44161-023-00311-0.
[49] Alexander, J.S., Elrod, J.W., 2002. Extracellular matrix, junctional integrity and matrix metalloproteinase interactions in endothelial permeability regulation. J Anat 200 (6), 561–574. https://doi.org/10.1046/j.1469-7580.2002.00057.x.
[50] Hendel, A., Hsu, I., Granville, D.J., 2014. Granzyme b releases vascular endothelial growth factor from extracellular matrix and induces vascular permeability. Lab Invest 94 (7), 716–725. https://doi.org/10.1038/labinvest.2014.62.
[51] Sluiter, T.J., van Buul, J.D., Huveneers, S., Quax, P.H.A., de Vries, M.R., 2021. Endothelial barrier function and leukocyte transmigration in atherosclerosis. Biomedicines 9 (4), 328. https://doi.org/10.3390/biomedicines9040328.
[52] EPA, U.S., 2012. Risk assessment forum. In: Benchmark Dose Technical Guidance, 20460. US Environmental Protection Agency, Washington, DC.
[53] Black, A., Luangphairin, N., Alfredo, K., 2025. The impact of the fourth regulatory determination on vulnerable populations. Environ Monit Assess 197 (3), 323. https://doi.org/10.1007/s10661-025-13689-0.
[54] Niu, S., Cao, Y., Chen, R., Bedi, M., Sanders, A.P., Ducatman, A., et al., 2023. A State-of-the-Science review of interactions of Per- and polyfluoroalkyl substances (PFAS) with renal transporters in health and disease: implications for population variability in PFAS toxicokinetics. Environ Health Perspect 131 (7), 76002. https://doi.org/10.1289/ehp11885.
[55] Verbeeck, R.K., 2008. Pharmacokinetics and dosage adjustment in patients with hepatic dysfunction. Eur J Clin Pharm 64 (12), 1147–1161. https://doi.org/10.1007/s00228-008-0553-z.
[56] Kim, A., Shin, D., Seo, Y., Kang, D., Min, Y.W., Kim, I.H., et al., 2025. Phase I study to evaluate the effect of hepatic impairment on pharmacokinetics and safety of tegoprazan, a potassium competitive acid blocker. Adv Ther 42 (3), 1570–1581. https://doi.org/10.1007/s12325-025-03127-5.
[57] Kurata, Y., Muraki, S., Hirota, T., Araki, H., Ieiri, I., 2022. Effect of liver cirrhosis on theophylline trough concentrations: a comparative analysis of organ impairment using Child-Pugh and MELD scores. Br J Clin Pharm 88 (8), 3819–3828. https://doi.org/10.1111/bcp.15333.
[58] Gouju, J., Legeay, S., 2023. Pharmacokinetics of obese adults: not only an increase in weight. Biomed Pharm 166, 115281. https://doi.org/10.1016/j.biopha.2023.115281.
[59] Amini-Salehi, E., Letafatkar, N., Norouzi, N., Joukar, F., Habibi, A., Javid, M., et al., 2024. Global prevalence of nonalcoholic fatty liver disease: an updated review Meta-Analysis comprising a population of 78 million from 38 countries. Arch Med Res 55 (6), 103043. https://doi.org/10.1016/j.arcmed.2024.103043.
[60] Gülden, M., Seibert, H., 2003. In vitro-in vivo extrapolation: estimation of human serum concentrations of chemicals equivalent to cytotoxic concentrations in vitro. Toxicology 189 (3), 211–222. https://doi.org/10.1016/s0300-483x(03)00146-x.
[61] Davis, J.A., Gift, J.S., Zhao, Q.J., 2011. Introduction to benchmark dose methods and U.S. Epa's benchmark dose software (BMDS) version 2.1.1. Toxicol Appl Pharm 254 (2), 181–191. https://doi.org/10.1016/j.taap.2010.10.016.